Electrospun Nanofiber Anodes of Low Platinum Loading for Hydrogen/Air PEM Fuel Cells

By

Amy Poynter

Thesis

Submitted to the Faculty of the

Graduate School of Vanderbilt University

in partial fulfillment of the requirements

for the degree of

MASTER OF SCIENCE

in

Chemistry

August 2014

Nashville, Tennessee

Approved:

Peter Pintauro, Ph.D.

David Cliffel, Ph.D.

ACKNOWLEDGEMENTS

I would like to thank my advisor, Professor Peter Pintauro, for the opportunity to be a part of the Pintauro group and his assistance and support in the completion of this thesis project. I would also like to thank Professor David Cliffel for the help he has provided as a part of my committee.

I am extremely appreciative of the members of the Pintauro group for their continued support throughout my time at Vanderbilt, particularly Matthew Brodt who taught me everything I know about proton exchange membrane fuel cells and was an extremely helpful (and patient) resource as I completed this research.

I would also like to extend a thank you to the many friends—new and old— and my family members who have been endlessly supportive during my time in graduate school through the good and the bad. Most importantly, I would like to thank Kevin Winter, my best friend at Vanderbilt from day one.

TABLE OF CONTENTS

Page

ACKNOWLEDGEMENTS ii

LIST OF TABLES iii

LIST OF FIGURES iv

Chapter

1. INTRODUCTION 1
   - 1.1 Motivation 1
   - 1.2 PEMFC Fundamentals 2
   - 1.3 Literature Review/Approaches 7
   - 1.4 Electrospun Nanofiber Electrodes 11
   - 1.6 Electrospinning Fundamentals 15

2 EXPERIMENTAL METHODS 18
   - 2.1 Fabrication of Electrospun Electrodes 18
   - 2.1.1 Scanning Electron Microscopy of Electrospun Mats 19
   - 2.2 Fabrication of Membrane-Electrode-Assemblies (MEAs) with Nanofiber Electrodes 20
   - 2.3 Fabrication of MEAs with a Thin Film Anode and Nanofiber Cathode 20
   - 2.4 Fuel Cell Tests 21

3 RESULTS AND DISCUSSION 22
   - 3.1 Nanofiber Electrospinning 22
   - 3.2 Characterization of Electrospun Nanofibers 25
   - 3.3 Performance with Conventional GDEs 27
   - 3.4 Effect of Pt Loading on MEA performance 35

4 CONCLUSIONS 45

5 SUGGESTIONS FOR FUTURE WORK 47

REFERENCES 49

LIST OF TABLES

Table 1. Electrospinning conditions used to fabricate nanofiber mats used for PEM fuel cell electrodes in the Pintauro group. 17
Table 2. Electrospinning conditions that were investigated to produce nanofibers that did not adhere to the collector drum. For all inks, the total polymer/particle content was 15 wt.%. and the Pt:Nafion:PAA weight ratio was fixed at 65:23:12. IPA: isopropanol, PrOH: propanol, MeOH: methanol, BuOH: butanol 22
Table 3. Summary of final electrospinning ink composition and electrospinning conditions. 25
Table 4. Current density at 0.6V for each anode of composition 65:23:12 Pt:Nafion:PAA and varied Pt loading for a 5cm^2 MEA with a Nafion 212 membrane, an electrospun cathode with Pt loading 0.10 mg$_{Pt}$/cm^2. Fuel cell operating conditions: 80◦C, 100% RH feed gases at ambient pressure, 125 sccm H_2 and 500 sccm air. 37
Table 5. Maximum power densities for MEAs with a nanofiber anode of composition 65:23:12 Pt:Nafion:PAA and different anode Pt loadings for a 5cm^2 MEA with a Nafion 212 membrane, and an electrospun cathode with Pt loading 0.10 mg$_{Pt}$/cm^2. Fuel cell operating conditions: 80◦C, 100% RH feed gases at ambient pressure, 125 sccm H_2 and 500 sccm air. 39
Table 6. Grams Pt required for 80 kW nanofiber MEA stack operating at 0.60V for different anode Pt loadings, where the cathode loading was fixed at 0.10 mg$_{Pt}$/cm^2. 40
Table 7. Grams Pt required for 80 kW nanofiber MEA stack operating at max power for different anode Pt loadings, where the cathode loading was fixed at 0.10 mg$_{Pt}$/cm^2. 41

LIST OF FIGURES

Figure 1. Schematic diagram of a typical hydrogen/air proton exchange membrane fuel cell (PEMFC). 3
Figure 2. Fuel cell stack design with bipolar plates, taken from reference.[6] 5
Figure 3. Voltage losses in a fuel cell and resultant polarization curve, taken from reference.[6] 6
Figure 4. a) Polarization curves for a H_2/air fuel cell employing MEAs with an electrospun cathode with the following cathode Pt loadings: (○) 0.1 mg/ cm^2 ,(solid line) 0.2 mg/ cm^2, and (Δ) 0.4 mg_{Pt}/cm^2 and with a decal cathode (dashed line) of 0.4 mg/ cm^2. (b) Normalized ECSA (electrochemical surface area) of (●) 0.4 mg_{Pt}/cm^2 electrospun cathode and (▲) 0.4 mg/ cm^2 decal cathode after voltage cycling (c) Polarization curves for a hydrogen/air fuel cell employing MEAs with an electrospun cathode (●) and a decal cathode (▲), both with cathode Pt loading of 0.4 mg/ cm^2, before (open) and after (solid) 1200 cycles. All plots are from reference 20. 13
Figure 5. A typical electrospinning setup, adapted from a reference showing a nanofiber mat of 65:23:12 Pt:Nafion:PAA weight ratio composition.[26] 16
Figure 7. Top-down scanning micrographs of nanofiber mats at different magnifications: a) 6000x, b) 3000x, c) 1500x, and d) 300x. 26
Figure 8. Histogram for nanofiber diameter distribution for the electrospun mat shown in Figure 7. 27
Figure 9. Polarization curves of MEAs with conventional GDE anodes of varying compositions. (▲) 70:30 Pt:Nafion weight ratio at 0.10 mg_{Pt}/cm^2 anode Pt loading, (•) 70:30 Pt:Nafion composition at 0.05 mg_{Pt}/cm^2 anode Pt loading, and (■) 65:23:12 Pt:Nafion:PAA composition at 0.10 mg_{Pt}/cm^2 anode Pt loading MEAs had electrospun cathode of composition 65:23:12 Pt:Nafion:PAA at 0.10 mg_{Pt}/cm^2. Fuel cell operating conditions: 80◦C, 100% RH feed gases at ambient pressure, 125 sccm H_2 and 500 sccm air. 28
Figure 10. Plots of power density vs. current density for MEAs with conventional GDE anodes of varying compositions. (▲) 70:30 Pt:Nafion weight ratio at 0.10 mg_{Pt}/cm^2 anode Pt loading, (•) 70:30 Pt:Nafion composition at 0.05 mg_{Pt}/cm^2 anode Pt loading, and (■) 65:23:12 Pt:Nafion:PAA composition at 0.10 mg_{Pt}/cm^2 anode Pt loading MEAs had electrospun cathode of composition 65:23:12 Pt:Nafion:PAA at 0.10 mg_{Pt}/cm^2. Fuel cell operating conditions: 80◦C, 100% RH feed gases at ambient pressure, 125 sccm H_2 and 500 sccm air. 30
Figure 11. Polarization curves of three MEAs with different anodes and the same nanofiber cathode. (•) Electrospun nanofiber anode of 65:23:12 Pt:Nafion:PAA weight ratio, (▲) conventional GDE anode of 70:30 Pt:Nafion composition, and (■) conventional GDE anode of 65:23:12 Pt:Nafion:PAA composition. All MEAs contained anodes of 0.10 mg_{Pt}/cm^2 loading and an electrospun nanofiber cathode of 0.10 mg_{Pt}/cm_2 loading and 65:23:12 Pt:Nafion:PAA weight ratio composition. Fuel cell operating conditions: 80◦C, 100% RH feed gases at ambient pressure, 125 sccm H_2 and 500 sccm air. 33
Figure 12. Power density vs. current density plots of three MEAs of different anodes. (•) Electrospun nanofiber anode of 65:23:12 Pt:Nafion:PAA weight ratio, (▲)

conventional GDE anode of 70:30 Pt:Nafion composition, and (■) conventional GDE anode of 65:23:12 Pt:Nafion:PAA composition. All MEAs contained anodes of 0.10 mg_{Pt}/cm^2 loading and an electrospun nanofiber cathode of 0.10 mg_{Pt}/cm_2 loading and 65:23:12 Pt:Nafion:PAA weight ratio composition. Fuel cell operating conditions: 80◦C, 100% RH feed gases at ambient pressure, 125 sccm H_2 and 500 sccm air. 34
Figure 13. Polarization curves for 5 cm^2 MEAs with a Nafion 212 membrane, an electrospun cathode of Pt loading 0.10mg_{Pt}/cm^2, and electrospun anodes of varying Pt loading. The anode Pt loading was: (•) 0.026, (□) 0.046, (o) 0.081, (■) 0.101, and (▲) 0.126 mg_{Pt}/cm^2 Pt loading. Fuel cell operating conditions: 80◦C, 100% RH feed gases at ambient pressure, 125 sccm H_2 and 500 sccm air. 36
Figure 14. Plots of power density vs. current density for 5cm^2 MEAs with a Nafion 212 membrane, an electrospun cathode of Pt loading 0.10mg_{Pt}/cm^2, and electrospun anodes of varying Pt loading. The anode Pt loading was (•) 0.026, (□) 0.046, (o) 0.081, (■) 0.101, and (▲) 0.126 mg_{Pt}/cm^2 Pt loading. Fuel cell operating conditions: 80◦C, 100% RH feed gases at ambient pressure, 125 sccm H_2 and 500 sccm air. 38
Figure 15. Polarization curves for a 5cm^2 MEA with a Nafion 212 membrane, an electrospun cathode and anode of 0.10 and 0.126 mg_{Pt}/cm^2 Pt loading, respectively at 40°C (▲), and 80°C(•). Fuel cell operating conditions: 100% RH feed gases at ambient pressure, 125 sccm H_2 and 500 sccm air.' 43
Figure 16. Polarization curves for a 5cm^2 MEA with a Nafion 212 membrane, an electrospun cathode and anode of 0.10 and 0.126 mg_{Pt}/cm^2 Pt loading, respectively at 40°C (▲) and 80°C (•). Fuel cell operating conditions: 100% RH feed gases at ambient pressure, 125 sccm H_2 and 500 sccm air. 43

1 INTRODUCTION

1.1 Motivation

The advent of the internal combustion engine paved the way for remarkable advances in transportation. As the world population continues to rise, it has become increasingly important to find sustainable sources of energy for transportation. Current transportation methods rely on fossil fuels, namely oil. In 2006, 86% of the total world energy consumption came from fossil fuels. This number is expected to increase from 500 exajoules to 720 exajoules by 2020, a 44% increase in 24 years. The use of fossil fuels has been known for many years to contribute to air and water pollution and increase atmospheric carbon dioxide concentrations, which contributes to the global greenhouse gas effect.[1] It is important to be prepared for potential energy shortages with environmentally cleaner, more sustainable sources of energy for transportation applications.

With the anticipation of a global energy crisis, finding alternative energy sources for transportation is increasingly important. One promising alternative is the hydrogen/air proton-exchange membrane fuel cell (PEMFC). Hydrogen/air PEMFCs have many attractive properties that put them at the forefront of fossil fuel alternatives for use in automotive/transportation applications. These properties include high energy conversion efficiency, no pollutant emissions, and the minimal use of moving parts. In an automobile, the fuel cell operates at a partial load (12-25% of maximum power) most of the time; under these conditions, efficiencies around 50% can be obtained.[2] In contrast, the energy conversion efficiency of internal combustion engines is around 20-35%.[3]

In addition to its higher efficiency, the hydrogen/air PEMFC is a much cleaner alternative to the combustion engine. While the internal combustion engine emits myriad harmful air pollutants, the only product of hydrogen/air PEMFC operation is water. Though fuel cells show great promise as an alternative to the internal combustion engine, several drawbacks including durability and cost, have limited commercial PEMFC viability. Because the electrodes in the membrane-electrode-assembly (MEA) typically use Pt on a carbon support as the catalyst for oxygen reduction and hydrogen oxidation, the occurrence of carbon corrosion will affect the long-term durability of the MEA, where carbon corrosion of the cathode electrode leads to a steady decrease in energy output. Carbon corrosion of cathodes occurs when the carbon support material is oxidized in the electrochemical environment of the fuel cell, leading to electrical isolation of Pt and a loss in available Pt surface area for reaction. The carbon in commercial Pt/C fuel cell catalysts reacts with water to form carbon dioxide, according to the following reaction[4]:

$$C + 2H_2O \rightarrow CO_2 + 4H^+ + 4e^-$$

An excess of water will lead to the corrosion of carbon, resulting in a decrease in Pt electrochemical surface area (ECA, the sites of electrochemically active Pt) and/or isolation of Pt sites, thus lowering fuel cell performance.[5] Another major barrier to commercialization of fuel cells is the high cost of the catalyst, so there is a critical need to lower the amount of Pt in an operating fuel cell.

1.2 PEMFC Fundamentals

Fuel cells are devices that convert the chemical energy of a fuel and oxidant directly into electrical energy (electricity). Electricity generation typically involves several conversion steps, but a fuel cell generates electricity in one electrochemical step that requires no

moving parts.[6] PEMFCs are classified based on the type of membrane that separates the anode and cathode (a proton exchange membrane) and the fuel that is employed, usually methanol or hydrogen.[7] The focus of this project is the H_2/air PEMFC. A schematic of this type of fuel cell is shown below in Figure 1.

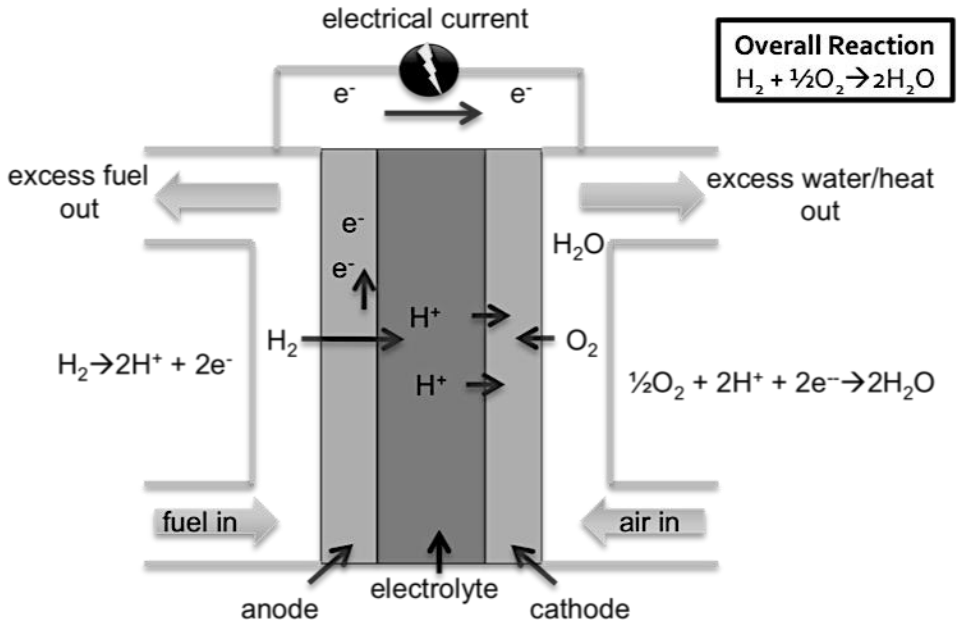

Figure 1. Schematic diagram of a typical hydrogen/air proton exchange membrane fuel cell (PEMFC).

In this system, H_2 gas is fed into the anode and air is fed to the cathode. At the anode, hydrogen is oxidized to produce protons and electrons.

$$H_2 \rightarrow 2H^+ + 2e^-$$

The electrons from the hydrogen oxidation reaction (HOR) travel through and external load to the cathode and the H^+ ions migrate to the cathode through the proton exchange membrane. Electrons, protons and oxygen react at the cathode to form water,

$$\frac{1}{2}O_2 + 2H^+ + 2e^- \rightarrow 2H_2O$$

Both the HOR and ORR require the presence of a catalyst for the reaction to occur. At present, the most commonly used catalyst is platinum. The first generation PEMFCs used unsupported Pt that required large amounts of precious metals, but the amount was reduced in the late 1990s when the use of supported Pt on carbon powder was employed. It is the active surface area of Pt that is most important in a fuel cell, rather than the mass of Pt. Thus, smaller Pt particles on a carbon support have a higher surface area and are more efficient at catalyzing the HOR and ORR.[6]

In a PEMFC, a cation-exchange membrane, typically Nafion, is placed between the anode and cathode to conduct protons, to serve as a barrier to prevent the mixing of reactant gases, and to prevent physical contact of the anode and cathode.[8] The gas diffusion layer (GDL) of a fuel cell electronically connects the catalyst layer and bipolar current collector plates. The GDL is typically a carbon based material, such as carbon paper or carbon cloth.[6] Membrane-electrode-assemblies (MEAs, which are membranes with attached catalyst layers) are stacked for an automobile fuel cell in order to obtain the desired power, in which case bipolar plates are placed between the anode and adjacent cathode[6], as can be seen in Figure 2.

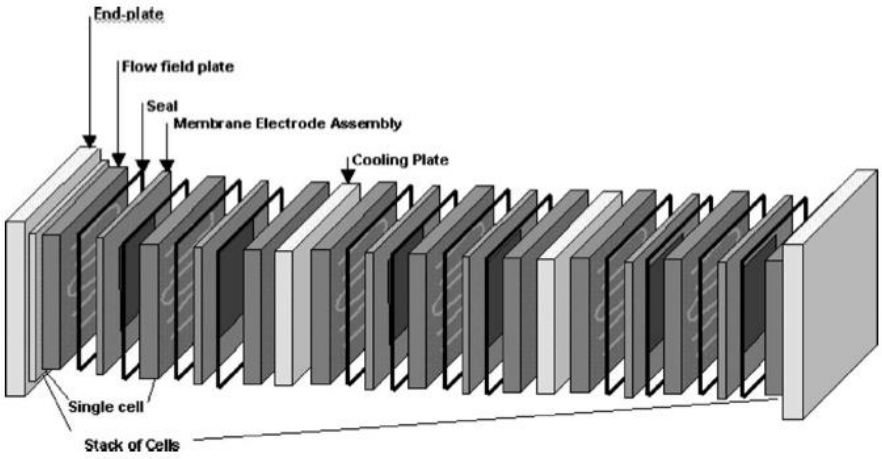

Figure 2. Fuel cell stack design with bipolar plates, taken from reference.[6]

The maximum theoretical (thermodynamic) voltage between the anode and cathode of a single cell operating in hydrogen/air is 1.23 V vs. standard hydrogen electrode (SHE) at ambient temperature and pressure. This value, however, cannot be achieved during current flow due to a voltage loss associated with the finite kinetics of the reactions and due to the fact that air contains only 18% oxygen. Reported OCVs in the literature for a hydrogen/air PEMFC are usually ~0.95V.[9]

The most common means of determining fuel cell performance is to examine voltage vs. current density polarization data. A polarization curve is a plot of cell potential (V) vs. current density (mA/cm^2). The three main types of power losses are activation polarization losses, ohmic losses, and concentration polarization losses. As shown in Figure 3, activation losses, (also known as kinetic losses), occur at high potentials and low current densities due to an activation energy barrier to the reduction of oxygen. At moderate current densities, ohmic losses are observed due to internal resistances such as the voltage required to drive protons across the membrane and into

and out of the catalyst layers. These losses follow Ohm's law, so there is a linear relationship with respect to current density.

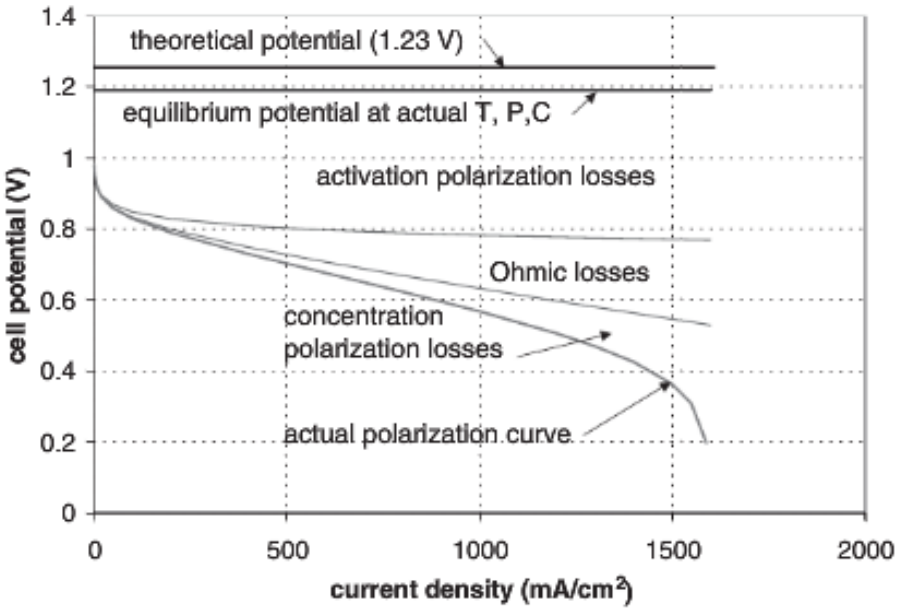

Figure 3. Voltage losses in a fuel cell and resultant polarization curve, taken from reference.[6]

At very high current densities, concentration polarization losses are the primary source of power loss. These losses are often caused by reactant depletion (i.e., mass transfer limitations). Because the anode is fed pure hydrogen gas during normal PEMFC operation, the cathode is the primary source of mass transport losses.[10]

From a polarization curve, the power density at varying voltages can be obtained by multiplying the current density by the voltage to obtain mW/cm^2. When looking at power density, both the maximum power density and the power density at either 0.60V or 0.65V are typically reported in the literature. In order to meet the packaging requirements for automotive applications, power densities of at least 800-900 mW/cm^2

are required. Additionally the maximum power density often occurs at cell voltages $\geq$0.65V, in which case the hydrogen conversion efficiency is high.[9] For the purposes of this thesis project, polarization curves and plots of power density versus current density were the primary means of assessing fuel cell performance with nanofiber and conventional gas diffusion electrodes.

Though PEM fuel cells provide a promising alternative to fossil fuels for use in automobiles, there are still several limitations that prevent the commercialization of fuel cell vehicles. The current PEMFC design uses relatively large amounts of platinum catalyst to drive both the anode and cathode reactions. According to an analysis published by the U.S. Department of Energy, the cost of the catalyst accounts for 49% of the total fuel cell stack cost, based on the manufacture of 500,000 PEMFC systems assuming a platinum loading of 0.153 mg_{Pt}/cm^2.[11] In addition, there are issues with electrode durability in PEMFC stacks during start/stop operation due to carbon corrosion (electrodes are typically made from Pt-on-carbon powder) .[12] In recent years, the focus of PEMFC research has been on reducing the amount of platinum required in the PEMFC electrodes and improving the durability of low Pt-loaded cathodes.

1.3 Literature Review/Approaches

The goal of reducing the amount of Pt required in a PEMFC is being approached in a variety of ways, including: increasing Pt mass activity through the use of alloys or core-shell nanostructures, improving mass-transport properties of current Pt-based cathodes, improving Pt utilization in current Pt-based electrodes and developing non-precious metal catalysts to drive the ORR at the cathode.[9] The first generation of PEMFCs utilized the hydrophobic polymer polytetrafluoroethylene (PTFE, Teflon) to bind platinum particles

to the gas diffusion layer. While these electrodes exhibited excellent long-term performance, the Pt loading required for this first generation electrode was 4 mgPt/cm^2, which is prohibitively high for scaleup.[13] An improved approach to MEA fabrication was found by using Nafion as the catalyst binder in fuel cell electrodes. In this thin-film approach, high power output can be obtained with low catalyst loadings, in the range of 0.4-0.8 mg. Thin film catalyst layers are spread onto a GDL or membrane from "inks" which consist of the catalyst and a Nafion emulsion in alcohol/water solvent. This type of electrode provides initial performance comparable to that of the PTFE-bound electrocatalysts layers while using a fraction of the Pt. The disadvantage is that long-term durability is not observed, due to the corrosion of the carbon on which the Pt is supported.[14]

Though using Nafion as a binder in the PEMFC electrodes allowed for a reduction in the amount of Pt required, 0.4 mg_{Pt}/cm^2 becomes a prohibitively high amount of Pt when the size of a fuel cell stack required in an automobile is taken into account (80-100 kW). As such, much research has been focused on further lowering the amount of Pt required.

In order to further reduce the amount of Pt in a fuel cell stack, research efforts have focused on modifying the structure of Pt nanoparticles. One means by which this has been attempted is by developing Pt-alloys. It has been found that Pt-alloys using Cr, Mn, Fe, Co, and Ni demonstrate a 2-4 fold increase in ORR activity, as compared to a conventional Pt/C catalyst. This is believed to be a result of a change in the structure of the electronic surface of Pt. Density functional theory (DFT) calculations performed by Nørskov[15] *et al.* have shown that alloys of Pt and Ni, Co, Fe, and Cr have smaller oxygen

binding energies than pure Pt. Though Pt-alloys have a high specific activity for ORR, issues/concerns remain with regards to catalyst deactivation due to leaching and/or dissolution of the base metal from the alloy surface in acidic solution. So improvements still need to be made on Pt-alloy catalyst durability.[16]

Another means by which researchers have attempted to reduce fuel cell costs by increasing Pt utilization is through replacing traditional carbon powders with multi-walled carbon nanotubes (MWCNTs) as support for the platinum catalyst. Growing carbon nanotube arrays on a carbon paper substrate and then electrodepositing Pt onto the MWCNTs results in a guaranteed electronic pathway from the Pt to the supporting electrode in the PEMFC. This prevents the isolation of carbon, which is an issue in conventional PEMFC electrodes and thus increase the utilization of Pt. MWNTs are particularly promising for this application because they have a very high surface area on which Pt nanoparticles can be deposited. For example, an MEA was prepared using two MWNT-carbon paper composite electrodes by immersing the two electrodes into a 5 wt% Nafion solution for 30 min and hot-pressing a Nafion 115 membrane between the two electrodes. The performance (power output) was found to be lower than that of a conventional Pt-based PEMFC electrodes with comparable Pt loading, which is suspected to be due to the larger size of the Pt particles on the CNTs as a result of the electrodeposition (25 nm vs. 2-3 nm of commercial Pt/C catalyst).[17]

Another major focus of PEMFC research is in eliminating the use of Pt (particularly in the cathode) altogether by replacing the Pt catalyst with a non-precious metal catalyst (NPMC). One type of NPMC that has shown promising catalytic activity for the ORR is the carbon-supported transition metal/nitrogen type of catalysts (M-N_x/C),

which consists of usually Co, Fe, Ni, or Mn, where x is usually 2 or 4. These types of catalysts are particularly promising because they can be synthesized using abundant, inexpensive precursors. These materials have been shown to catalyze the ORR in both alkaline and acidic environments, though the earlier structures were found to decompose in the presence of acid, resulting in a loss of catalytic activity. A breakthrough in NPMC technology occurred when it was discovered that high temperature heat treatment procedures could be used in the synthesis of the catalysts to increase the concentration of available active sites for the ORR to occur and to also improve the stability of the catalyst. Various M-N_x/C structures have been synthesized from a variety of precursors. Research has shown that the only requirements in the structure for ORR catalytic activity are proper coordination of the metal and a nitrogen-containing carbon support. Pyrolized M-N_x/C structures have exhibited a catalytic activity and stability close to their Pt/C counterparts, however their volumetric activity still does not reach the 2010 DOE target of 130 A/cm^3 or the 2015 DOE target of 300 A/cm^3 so more development is needed for these types of catalysts. Additionally, the durability tests performed on these M-N_x/C structures were run at low current (low power), which is not representative of the actual fuel cell environment, so improving the stability of these catalysts is also vital.[18]

In NPMCs, it is often found that a particular structure demonstrates respectable performance and low durability or vice versa. For example, the Zelenay group synthesized a polypyrrole-Co-C system that showed performance durability but had relatively low oxygen reduction activity. In order for commercialization to be feasible, a catalyst must show that it has both good performance and good stability. The Zelenay group has found that polyaniline(PANI)-derived NMPCs show the greatest promise,

demonstrating both promising oxygen reduction activity and respectable performance durability. Both metal-free PANI-C and transition metal-containing PANI-C catalysts were tested in this study. Fuel cell polarization data demonstrated that the addition of a transition metal greatly improves catalytic activity and that PANI-Fe-C exhibits higher ORR rates than PANI-Co-C. The highest performing PANI-derived catalyst was a mixed-metal PANI-FeCo-C material, which exhibited a maximum power density of 0.55 W/cm^2 at 0.38V and maintained its activity when mixed with Nafion ionomer in a fuel cell electrode. In addition, when subjected to a 700-hour fuel-cell performance test at a constant cell voltage of 0.4 V, the stability of the PANI-Pt alloy catalyst was very good, with a current density decline of only 3% over a period of 700 hours. While these PANI-derived NPMCs show great promise, Pt-based catalysts continue to exhibit higher performance.[19]

1.4 Electrospun Nanofiber Electrodes

Research efforts continue to focus on improving the Pt utilization in Pt-based fuel cell electrodes in order to retain their excellent performance (power output) while reducing the amount of Pt required in the electrode. One means by which the amount of Pt can be more effectively utilized is by incorporating Pt/C powders into electrospun polymeric nanofibers. Because of their high surface to volume ratio, there is better contact between Pt and the reactant gases in the fuel cell. Electrospun nanofiber cathodes have been studied and evaluated by Pintauro and coworkers. In 2011, Zhang and Pintauro[20] fabricated electrospun nanofiber-electrode mats and then tested them as the cathode in H_2/air and H_2/O_2 PEMFCs, where the catalyst binder was a mixture of Nafion and poly(acrylic acid) (henceforth abbreviated as PAA). They reported very high power

densities at low Pt loading (524 mW/cm^2 at 0.6V at 80°C and ambient pressure with 0.1 mg$_{Pt}$/cm^2), vs. 519 mW/cm^2 for a conventional MEA with a cathode catalyst loading 4x higher (0.4 mg$_{Pt}$/cm^2). They also reported a mass activity (current per mg Pt) that rivals the best cathodes in the literature (0.23 A/mg$_{Pt}$ at 0.9V in an 80°C H_2/O_2 fuel cell). In addition, after a catalyst durability test (1200 voltage cycles from 0.6-1.2V at 20mV/s), the electrospun cathode showed significantly less degradation in performance (i.e., less Pt and/or carbon corrosion) as compared to a decal-processed cathode containing Pt/C and Nafion at the same Pt loading.[20] Typical hydrogen/air fuel cell polarization curves for nanofiber cathodes (from reference 20) are shown in Figure 4a, where it can be seen that the performance of MEAs with electrospun nanofiber cathodes of Pt loading 0.1-0.4 mg$_{Pt}$/cm^2 outperformed an MEA with a standard decal processed cathode of 0.4 mg$_{Pt}$/cm^2. In this test, the anode was held constant for all MEAs. The current density of the MEA with an electrospun cathode of 0.1 mg$_{Pt}$/cm^2 loading was slightly better than the MEA with a decal processed cathode of 0.1 mg$_{Pt}$/cm^2 at 0.6V, but the MEA with an electrospun cathode of 0.4 mg$_{Pt}$/cm^2 loading exhibited a significantly higher current density and power density than the MEA with decal processed cathode at 0.6V (519 mW/cm^2 vs. 662 mW/cm^2). Figure 4b shows the change in the normalized electrochemical surface area (ECSA) versus number of cycles during a carbon corrosion voltage cycling experiment. The ECSA is the surface area of the cathode that can be accessed by reactant gases and can be used to catalyze the ORR, so a higher ECSA demonstrates higher Pt utilization. ECSA is measured by means of cyclic voltammograms, as described in references 21-24. Figure 4b shows that after 1200 voltage cycles, the decal cathode had lost 75% of its initial ECSA, whereas the decline of

the ECSA of the electrospun nanofiber cathode was much less severe—declining only to the initial ECSA of the decal cathode. Because a higher ECSA yields higher Pt utilization and thus better performance, the performance of the MEA with electrospun nanofiber cathode was much better than the performance of the MEA with the decal cathode. Figure 4c shows polarization curves after 1200 cycles for an MEA with an electrospun cathode and an MEA with a decal cathode, both of 0.4 mg_{Pt}/cm^2 loading. As can be seen, the current density decline of the MEA with an electrospun cathode (is far less than that of the MEA with the decal cathode due to the retention of ECSA in the electrospun nanofiber cathode.

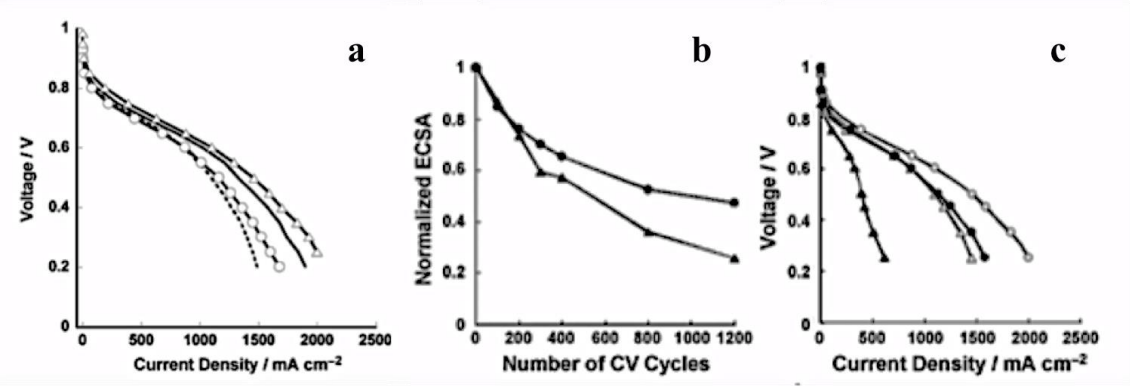

Figure 4. a) Polarization curves for a H_2/air fuel cell employing MEAs with an electrospun cathode with the following cathode Pt loadings: (○) 0.1 mg/ cm^2 ,(solid line) 0.2 mg/ cm^2, and (Δ) 0.4 mg_{Pt}/cm^2 and with a decal cathode (dashed line) of 0.4 mg/ cm^2. (b) Normalized ECSA (electrochemical surface area) of (●) 0.4 mg_{Pt}/cm^2 electrospun cathode and (▲) 0.4 mg/ cm^2 decal cathode after voltage cycling (c) Polarization curves for a hydrogen/air fuel cell employing MEAs with an electrospun cathode (●) and a decal cathode (▲), both with cathode Pt loading of 0.4 mg/ cm^2, before (open) and after (solid) 1200 cycles. All plots are from reference 20.

In a follow-on study, Brodt and Pintauro[24] performed a more in-depth analysis of electrospun cathodes, using Pt/C powder catalyst and a binder of Nafion and PAA. In particular, the effect of cathode Pt loading (0.025 mg_{Pt}/cm^2 to 0.110 mg_{Pt}/cm^2) and fuel cell operating conditions on power output were assessed. The nanofiber MEAs performed very well, with only an 15% drop in power output at 0.65V when the Pt loading was reduced from 0.110 to 0.065 mg_{Pt}/cm^2 (437 vs. 513 mW/cm^2 at 0.65V) In addition, the nanofiber cathode with 0.0645 mg_{Pt}/cm^2 Pt loading was shown to outperform a decal cathode with a Pt loading of 0.10 mg_{Pt}/cm^2 under the same operating conditions.

1.5 Objectives of Research

A major focus of the PEMFC scientific community and Pintauro's research group has been on reducing the amount of Pt required at the cathode in a hydrogen/air PEMFC, where the ORR takes place. Prior studies did not focus on the effect of Pt loading on anode performance. The objective of the present M.S. research project is to expand upon the results found by Zhang, Brodt, and Pintauro by investigating the effect of anode Pt loading on fuel cell performance. Additionally, nanofiber anode MEA performance results will be compared to that with a standard decal anode where the anode catalyst binder is either Nafion or Nafion/PAA (i.e., the same binder as that used in the electrospun nanofibers). Because of the high surface area of electrospun nanofibers, it is hypothesized that the anode Pt loading could be appreciably reduced without a drastic drop in fuel cell power output, which would be highly desirable from a MEA capital cost and commercialization standpoint.

1.6 Electrospinning Fundamentals

Electrospinning can be used to create nanofiber fuel cell electrodes that have a very high surface area, where there is inter-fiber and intra-fiber porosity in the final nanofiber electrode mat.[24] During the process of electrospinning, a charged polymer jet is formed by applying an electrostatic voltage to a spinneret tip that is attached to a reservoir (e.g., a syringe) containing a viscous polymer solution. With a sufficiently high applied potential (usually several kV), electrostatic forces overwhelm surface tension forces and a Taylor cone is formed from the solution as it emerges from the spinneret tip. A fiber jet of very small diameter is emitted from the Taylor cone and travels to a grounded rotating drum collector. Solvent evaporates from the fiber as the jet travels to the collector, during which time the filament jet elongates, resulting in a further decrease in fiber diameter. Randomly aligned nanofibers are collected as a mat of uniform thickness and fiber volume fraction on the drum. A schematic of a typical electrospinning setup is shown below in Figure 5. The entirety of the electrospinning apparatus, shown in Figure 5, is contained in a plexiglass chamber, where the humidity can be controlled.

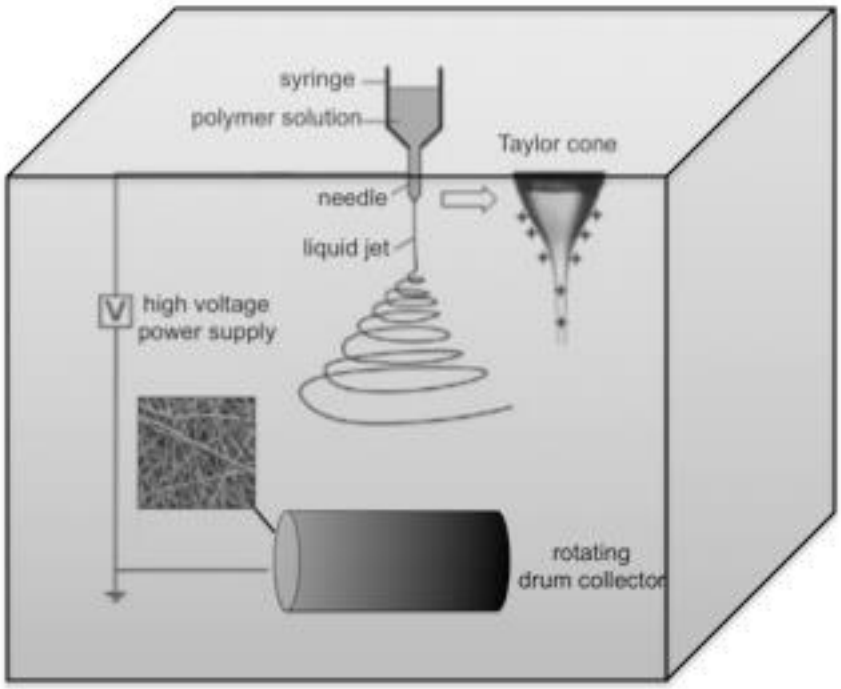

Figure 5. A typical electrospinning setup, adapted from a reference showing a nanofiber mat of 65:23:12 Pt:Nafion:PAA weight ratio composition.[26]

In order to produce a high-quality electrospun nanofiber mat, there are several operating conditions to be examined and properly set: the total polymer and catalyst concentration in the electrospinning fluid, the need for an electrospinnable carrier polymer such as polyacrylic acid (PAA) or polyethylene oxide (PEO) when Nafion perfluorosulfonic acid is the proton conducting catalyst powder binder, the applied voltage, the spinneret-to-collector distance, solution flow rate, and the humidity in the electrospinning chamber. Although finding the appropriate conditions to electrospin nanofibers is not a trivial task, many polymers of proper molecular weight can be electrospun, as well as polymer/particle systems.[1, 20, 25-27] The electrospinning conditions used by Zhang and Brodt to electrospin the aforementioned nanofiber electrode mats are

shown in Table 1, along with the electrospinning conditions used for the data presented in the current study. The electrospinning conditions in Table 1 yield very similar nanofiber mats; changes in conditions are due to optimization of conditions and modifications in electrospinning ink composition, which requires a modification in electrospinning conditions.

Table 1. Electrospinning conditions used to fabricate nanofiber for PEM fuel cell electrodes in the Pintauro group.

	Applied Voltage (kV)	**Relative Humidity (%)**	**Spinneret-to-Collector Distance (cm)**	**Solution Flow Rate (mL/hr)**
Zhang[20]	6	ambient	9	1.5
Brodt[25]	9	ambient	10	1
Poynter	15	50%	8	1

2 EXPERIMENTAL METHODS

2.1 Fabrication of Electrospun Electrodes

Nafion/PAA nanofiber mat electrodes were fabricated using inks prepared by mixing Johnson Matthey Company HiSpec 4000 Pt/C powder (40% Pt on carbon black), Nafion perfluorosulfonic acid cation exchange resin (20 wt.% in a n-propanol/water solution, from Ion Power), and poly(acrylic acid) (MW=450 kDa from Aldrich) in an isopropanol/water solution. In the ink, PAA acts as a carrier polymer to provide sufficient polymer chain entanglements so that Nafion polymer can be electrospun without the formation of unwanted droplets and beads.[26] A suspension of the 20% Nafion solution and catalyst in a water/acetone mixed solvent (25 wt.% acetone and 75 wt./% water) was first sonicated for 60 minutes with intermittent mechanical stirring before the addition of PAA and acetone. The entire mixture was then stirred for approximately 24 hours. The total polymer/powder content of the electrospinning ink was 15 wt.% with a Pt/C:Nafion:PAA weight ratio of 65:23:12; this composition was identical to that used by Brodt in his 2013 paper.[25] For electrospinning, the ink was drawn into a 3-mL syringe attached to a 22-gauge stainless steel needle spinneret, with the spinneret tip polarized to a potential of 15 kV relative to a grounded stainless steel rotation drum collector that oscillated horizontally for improved uniformity of the nanofiber mat thickness. The spinneret to collector distance was fixed at 9 cm and the flow of ink for all experiments was 1.0 mL/h (the flow rate was controlled by a syringe pump). Electrospinning was performed at room temperature inside a plexiglass chamber where the relative humidity was controlled and maintained constant at 50%. To change the Pt content (loading) of a nanofiber anode, the electrospinning duration time was increased, using a fixed ink

composition and constant electrospinning conditions. So nanofiber anodes of different Pt loading were fiber mats of different thickness, where the fiber composition (the relative amounts of Nafion, PAA, and catalyst) was held constant and where the electrospinning conditions were fixed so that the fibers were of the same average diameter.

2.1.1 Scanning Electron Microscopy of Electrospun Mats

Nanofibers were imaged using a Hitachi S4200 high-resolution scanning electron microscope (SEM). To obtain these images, the nanofiber mat was lightly pressed at room temperature onto SEM tape and sputter-coated with gold to increase conductivity and thus improve contrast in the SEM images. Top-down scanning electron micrographs (SEMs) were collected at magnifications of 6000x, 3000x, 1500x, and 300x. The SEMs were then used to determine the average fiber diameter in a nanofiber mat. Nanofiber diameter was obtained by first using the ImageJ software to measure the length of the scale bar. A sampling of 100 fibers on this same SEM was then manually selected and the diameter was measured and compared to the measure of the length of the scale bar. For each nanofiber, the diameter was measured in approximately 20 locations across the fiber (to obtain a more accurate measurement since fiber diameter is not perfectly uniform across the fiber). These measurements were then used to create a histogram showing distribution of nanofiber diameter.

2.2 Fabrication of Membrane-Electrode-Assemblies (MEAs) with Nanofiber Electrodes

MEAs with nanofiber electrodes were fabricated by sandwiching a Nafion 212 membrane between an electrospun anode mat and electrospun cathode mat. The geometric area of the electrodes was 5 cm^2. The electrodes were hot-pressed onto the membrane at 140°C and 4000 pounds of pressure for 1 minute (after allowing the membrane and electrodes to pre-heat at 140°C for 10 minutes). The platinum content of each electrode was calculated from the total weight of the mat, knowing the weight-fraction of Pt used in the electrospinning ink.

2.3 Fabrication of MEAs with a Thin Film Anode and Nanofiber Cathode

Three conventional MEAs were fabricated using a gas diffusion electrode (GDE) as the anode and an electrospun nanofiber mat as the cathode. A standard GDE anode of 77:23 wt.% Pt:Nafion was made by mixing Johnson Matthey HiSpec catalyst 4000 catalyst powder with a 20% Nafion solution from Aldrich and then painting the ink onto Sigracet® GDL 25 BC carbon paper (from Ion Power), where the final Pt loading was 0.1 mg_{Pt}/cm^2. The carbon paper electrode was then dried in an oven at 70°C for 30 minutes. Two catalyst coated GDE anodes of the same composition as the electrospun nanofibers (with a 65:23:12 wt.% of Pt:Nafion:PAA) were created in the same manner, with Pt loadings of 0.10 and 0.05 mg_{Pt}/cm^2. All GDE anodes were hot-pressed onto a Nafion 212 membrane with an electrospun nanofiber cathode (where the wt.% of Pt:Nafion:PAA was 65:23:12 and the total cathode Pt loading was fixed at 0.10 mg_{Pt}/cm^2

loading). The electrode hot pressing conditions were: at 140°C and 0 psi for 10 minutes (a pre-heat step) and then 4000 psi at 140°C for 1 minute.

2.4 Fuel Cell Tests

In order to assess electrode performance, fuel cell polarization curves were obtained using a Scribner Series 850e test station, with a fuel cell test fixture containing single anode and cathode serpentine flow channels. All MEAs were tested in the same way. Experiments in H_2/air were performed at 80°C under fully humid feed gas conditions with flow rates of 0.125 sccm H_2 and 0.500 sccm air. Prior to data collection, the MEAs were conditioned by alternating between two minutes of low current (0.75A) and two minutes of low voltage (0.2V) at 80^{o}C for sufficient time until a steady power output from the MEA was achieved. This normally occurred after approximately four hours. Prior to collecting polarization data, the MEA was further pre-conditioned by repeating 20 times a cyclic voltammetry (CV) scan, from 0.04 V to 0.9 V at a scan rate of 100 mV/s (the Gamry potentiostat was used to perform the CVs). Polarization curves were then collected after a brief wait for the system to re-stabilize (approximately one minute).

3 RESULTS AND DISCUSSION

3.1 Nanofiber Electrospinning

The method described by Brodt[25] for electrospinning particle/polymer nanofiber mat fuel cell electrodes was used in the initial electrospinning experiments. Unfortunately, this method did not work well. Nanofibers were produced but they adhered to the foil on the collector drum and were difficult to remove. MEAs made from these mats were not durable, as determined in follow-on fuel cell tests. The poor electrospinning results were attributed to: (1) the temperature/humidity in the electrospinning chamber during mat fabrication and/or (2) some contamination of the alcohol solvent used in the electrospinning ink. In an effort to produce more "fluffy" (non-adhering) nanofibers that could easily be removed from the collector drum, a variety of electrospinning conditions were investigated, as listed in Table 2.

Table 2. Electrospinning conditions that were investigated to produce nanofibers that did not adhere to the collector drum. For all inks, the total polymer/particle content was 15 wt.%. and the Pt:Nafion:PAA weight ratio was fixed at 65:23:12. IPA: isopropanol, PrOH: propanol, MeOH: methanol, BuOH: butanol

Solvent Composition	**Voltage (kV)**	**Humidity (%)**	**Result**
58:39:3 Water:IPA:PrOH	12	25	Sprayed droplets
58:39:3 Water:IPA:PrOH	15	25	Sprayed droplets
58:39:3 Water:IPA:PrOH	15	25	Adhered fibers
58:21:18:3 Water:IPA:MeOH:PrOH	15	25	Sprayed droplets (with needle clogging)

58:21:18:3 Water:IPA:MeOH:PrOH + 2 drops BuOH	15	25	Adhered fibers
58:37:3:2 Water:Acetone:PrOH:IPA	15	25	Adhered fibers
58:37:3:2 Water:Acetone:PrOH:IPA	15	50	Non-adhered fibers (good)

When determining what solvent types and compositions to examine for the electrospinning ink, two factors were considered: solvent boiling point and the relative humidity in the electrospinning chamber. The solvent boiling point is very important in selecting the correct ink composition, because nanofiber formation is strongly affected by the evaporation rate and viscosity of the solvent. The solvent must evaporate before the fiber contacts the drum, otherwise electrospray droplets or electrospun ribbon structures will be created. Conversely, if the solvent evaporates too quickly, the dry fibers will lack sufficient surface charge to deposit on the grounded collector drum and will deposit on surfaces inside the electrospinning chamber other than the drum.

Water can absorb into the fibers as they move towards the collector, so the relative humidity in the electrospinning chamber can also affect the rate at which the nanofibers dry as they make their way to the collection drum. If the relative humidity of is too high, there will still be water in the fibers when they reach the grounded collector drum resulting in electrospray droplets or electrospun ribbon structures. Similarly, if the humidity of the electrospinning chamber is too low, the fibers will dry prior to reaching the collector drum and deposit on surfaces other than the drum (much like in the case of the solvent in the ink drying too quickly). For the purposes of this study, the solvent and

the relative humidity of the box were the primary factors that were changed to make a well-formed and useable anode mat.

The voltage was fixed at ~15V because at this voltage, a Taylor cone formed (the precursor to nanofiber formation) for all solvent types and compositions. Additionally, it was found that the optimum stirring time for all ink compositions was 24 hours. A stirring time of 12 hours did not provide sufficient time for the solution to properly mix, whereas a stirring time of 48 hours resulted in the evaporation of enough solvent to cause the needle spinneret to clog during electrospinning.

Methanol was initially added to the electrospinning ink in an attempt to lower the boiling point of the solvent, however there were problems with droplet formation and the needle clogging when a sample with a Water:IPA:MeOH:PrOH solvent (58:21:18:3 weight ratio) was tested. Next, the solution composition was modified by adding a few drops of butanol to the 5 ml ink sample, in an attempt to slightly raise the boiling point of the solvent so that the needle would not clog but the fibers would be dry upon contacting the collector drum. Unfortunately, this did not work; the fibers were adhering to the foil on the collector drum.

In a further attempt to make a nanofiber mat of "fluffy" non-adhered fibers that could easily be removed from the collector drum and incorporated into an MEA, the isopropanol (IPA) in the ink (that amount of isopropanol that was added to the Nafion solution and catalyst during ink preparation) was replaced with acetone to give a composition of 58:37:3:2 Water:Acetone:PrOH:IPA. The boiling point of acetone is considerably lower than that of isopropanol (56 vs. 82.5^{o}C). In this case, there were no problems with the needle clogging as in the solution containing IPA and methanol,

however there were still problems with the fibers sticking to the foil. At this point, the relative humidity of the system was raised from 25% to 50%. Non-adhering (fluffy), high-quality electrospun mats with well-formed nanofibers were obtained at this higher humidity, using an ink with a particle/polymer content of 15 wt.% a solvent of water:acetone:propanol:IPA at a 58:37:3:2 weight ratio, and a Pt:Nafion:PAA weight ratio composition of 65:23:12. The electrospinning was carried out at 15 kV applied potential, a spinneret-to-collector distance of 8 cm, and a solution flow rate of 1.0 mL/hr.

Table 3. Summary of final electrospinning ink composition and electrospinning conditions.

Ink Composition	**Applied Voltage (kV)**	**Relative Humidity (%)**	**Spinneret-to-Collector Distance (cm)**	**Solution Flow Rate (mL/hr)**
58:37:3:2 Water:Acetone:PrOH:IPA	15	50%	8	1

The final electrospinning ink composition and electrospinning conditions are summarized in Table 3. All inks were stirred for approximately 24 hours prior to electrospinning. Typically, an electrospinning time of 40 minutes was required to fabricate an anode mat 17 cm x 17 cm in area with a Pt loading of 0.1 mg_{Pt}/cm^2.

3.2 Characterization of Electrospun Nanofibers

Scanning electron micrographs of a nanofiber mat with Pt loading of 0.10 mg_{Pt}/cm^2 are shown at different magnifications in Figure 7.

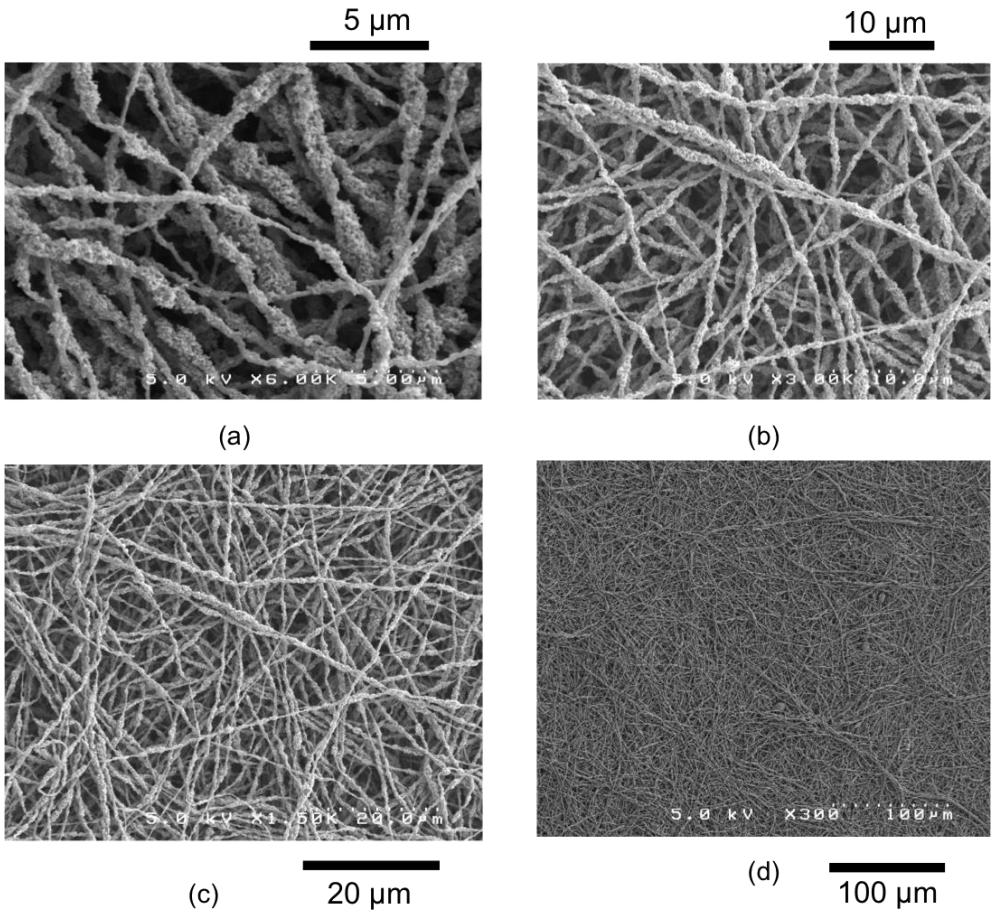

Figure 6. Top-down scanning micrographs of nanofiber mats at different magnifications: a) 6000x, b) 3000x, c) 1500x, and d) 300x.

As can be seen, the nanofibers are distributed quite evenly across the mat and are somewhat uniform in diameter. A histogram showing the distribution of nanofiber diameter for the nanofiber mat is presented in Figure 8. For the results in Figure 8, the average nanofiber diameter was found to be 594±51 nm with a 95% confidence interval. The mat morphology shown in Figure 7 and the fiber diameter distribution in Figure 8 were typical for all nanofiber anodes used in this study. It should also be noted that the average fiber diameter for the mat in Figure 7 (594 nm) was essentially the same as that for a nanofiber cathode mat (589 nm), as reported in the literature by Brodt et al.[25]

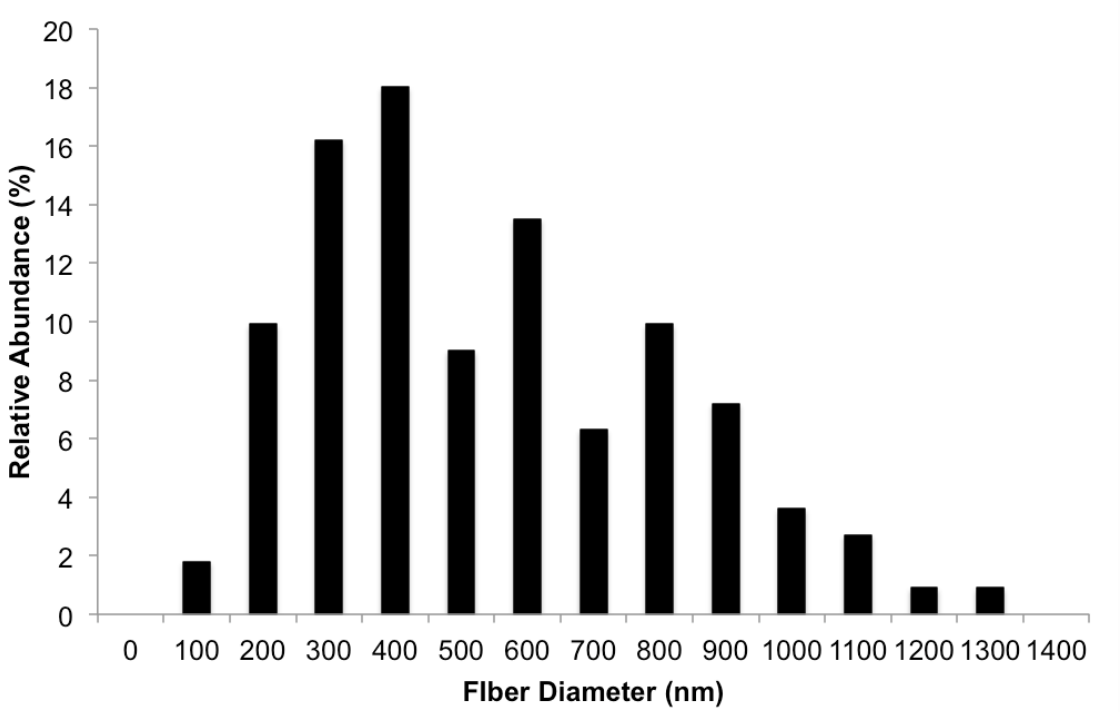

Figure 7. Histogram for nanofiber diameter distribution for the electrospun mat shown in Figure 7.

3.3 Performance with Conventional GDEs

A series of fuel cell tests were performed in order to compare the performance of an electrospun nanofiber anode MEA to the performance of an MEA with a conventional/standard GDE (gas diffusion electrode) anode. The conventional GDE anode tests were performed first. Three MEAs were made with GDE anodes. All of these MEAs had an electrospun cathode with a Pt loading 0.10 mg_{Pt}/cm^2. Two MEAs with GDE anodes had a catalyst:binder (Pt:Nafion) weight ratio of 70:30 and were of 0.10 and 0.05 mg_{Pt}/cm^2 Pt loading. The other MEA tested contained an anode with 0.10 mg_{Pt}/cm^2 loading and the Pt:Nafion:PAA weight ratio was 65:23:12 (the same binder composition and Pt:Nafion:PAA ratio as an electrospun nanofiber mat anode). Polarization curves and power density vs. current density plots of the three MEAs with conventional GDE

anodes (for fuel cell operation with hydrogen/air at 80°C, 100% relative humidity, and ambient pressure) are shown in Figures 9 and 10, respectively.

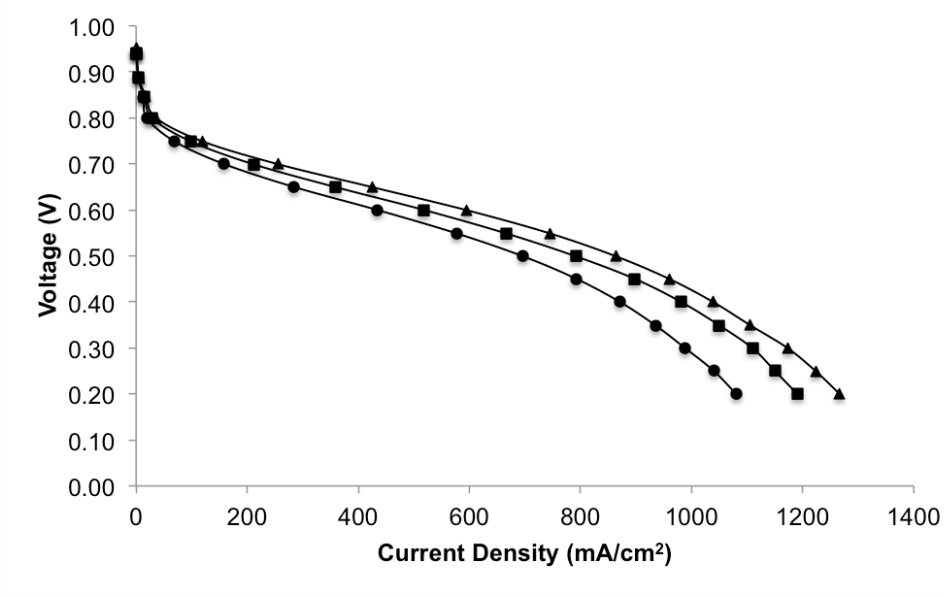

Figure 8. Polarization curves of MEAs with conventional GDE anodes of varying compositions. (▲) 70:30 Pt:Nafion weight ratio at 0.10 mg_{Pt}/cm^2 anode Pt loading, (•) 70:30 Pt:Nafion composition at 0.05 mg_{Pt}/cm^2 anode Pt loading, and (■) 65:23:12 Pt:Nafion:PAA composition at 0.10 mg_{Pt}/cm^2 anode Pt loading MEAs had electrospun cathode of composition 65:23:12 Pt:Nafion:PAA at 0.10 mg_{Pt}/cm^2. Fuel cell operating conditions: 80◦C, 100% RH feed gases at ambient pressure, 125 sccm H_2 and 500 sccm air.

The polarization curves in Figure 9 show the observed voltage vs. current density dependence for MEAs with two conventional GDE anodes with different binder compositions and the same Pt loading (0.10 mg_{Pt}/cm^2), as well as a conventional GDE electrode of 70:30 Pt:Nafion composition with an anode Pt loading of 0.05 mg_{Pt}/cm^2. The difference between the two anodes of 0.10 mg_{Pt}/cm^2 is that one contained PAA and the other did not. Because PAA must be used as a binder to electrospin nanofiber mats to be used as anodes, conventional GDEs were tested both with and without PAA to

determine the effect of PAA on MEA (anode) performance. The polarization data above is very similar to the data collected by Brodt et al. for an MEA with an electrospun cathode of 0.10 mg_{Pt}/cm^2 Pt loading and a 0.40 mg_{Pt}/cm^2 GDE anode with a weight ratio composition of 77:23 for Pt:Nafion, in which a current density of ~580 mA/cm^2 was observed at 0.60V[25] (vs. 594 mA/cm^2 for the data plot in Figure 9 with a 70:30 Pt/C:Nafion anode. There was a 27% decrease in current density at 0.60V when the anode Pt loading was lowered from 0.10 mg_{Pt}/cm^2 to 0.05 mg_{Pt}/cm^2 for a conventional GDE anode MEA with a 70:30 Pt/C:Nafion composition. As can be seen in Figure 9, the MEA with an anode with no PAA reaches a higher current density at 0.60V than the MEA with a Nafion/PAA binder anode at the same Pt loading. The MEA with a PAA-containing anode reaches a current density of 557 mA/cm^2 at 0.60 V whereas the MEA with an anode that does not contain PAA reaches a current density of 595 mA/cm^2 at the same voltage. The slopes of all MEAs in the polarization curve are very similar, which suggests that the ohmic resistance through the membrane and the contact resistance between the membrane and electrodes are very similar for all MEAs.

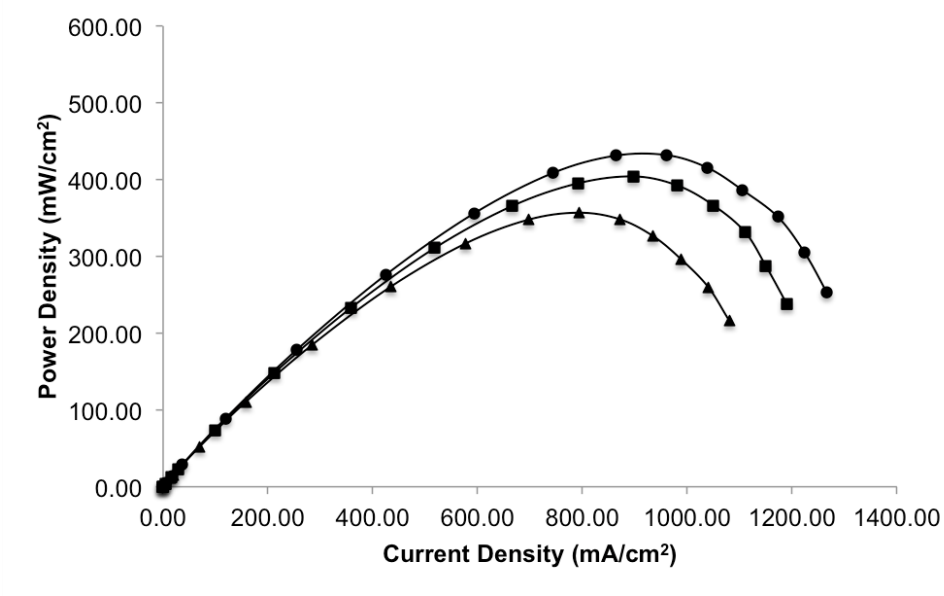

Figure 9. Plots of power density vs. current density for MEAs with conventional GDE anodes of varying compositions. (▲) 70:30 Pt:Nafion weight ratio at 0.10 mg_{Pt}/cm^2 anode Pt loading, (•) 70:30 Pt:Nafion composition at 0.05 mg_{Pt}/cm^2 anode Pt loading, and (■) 65:23:12 Pt:Nafion:PAA composition at 0.10 mg_{Pt}/cm^2 anode Pt loading MEAs had electrospun cathode of composition 65:23:12 Pt:Nafion:PAA at 0.10 mg_{Pt}/cm^2. Fuel cell operating conditions: 80◦C, 100% RH feed gases at ambient pressure, 125 sccm H_2 and 500 sccm air.

The MEA containing PAA in Figure 9 exhibited slightly lower performance, which is consistent with results previously observed in the Pintauro group. Previous work from Brodt et al.[29] has shown that the absence of PAA or having too little PAA in the electrospinning ink results in the formation of electrosprayed droplets rather than nanofibers, whereas an excess of PAA in the nanofiber composition results in lowered fuel cell performance due to lowered poor ionic and electronic conductivity in the nanofibers. When PAA is added to an anode ink, the wt% of Nafion and Pt in the ink must both be slightly lowered so that the proper viscosity for electrospinning is

maintained without drastically lowering either the Pt or Nafion in the solution. Research has shown that adding PAA to Nafion results in a decrease in conductivity of the nanofibers[30], which leads to diminished fuel cell performance. This can be seen in the experimental results in Figures 9 and 10. The data shows that the power density ratio for the conventional GDE MEA of 0.10 mg_{Pt}/cm^2 anode Pt loading with 70:30 Pt:Nafion composition compared to the MEA with a composition of 65:23:12 Pt:Nafion:PAA at the same anode Pt loading is 1.15 at 0.60V and 1.06 at max power. This suggests that the addition of PAA to the anode composition results in a slight decrease in performance, as was expected, however the extent to which the fuel cell performance was diminished was significantly less than what was found by Brodt et al[29] when assessing the effect of PAA in the cathode on MEA performance. In this study, the performance of two MEAs with different GDE cathode compositions were compared: a cathode of 67:33 Pt:Nafion weight ratio and 72:13:15 Pt:Nafion:PAA weight ratio. In this case, the power density ratio comparing the Pt:Nafion and Pt:Nafion:PAA was 1.24 and 1.19 at 0.60V and max power, respectively. Although the two sets of results cannot be compared directly because the weight ratio compositions of the nanofibers vary between studies, the data suggests that the effect on fuel cell performance is less severe when PAA is added to the anode rather than the cathode. Additionally, the power density ratio comparing conventional GDE anode MEA at 0.10 mg_{Pt}/cm^2 and 0.05 mg_{Pt}/cm^2 is 1.22 at 0.60V and 1.21 at max power, suggesting that an approximately 20% drop in power is observed when the Pt loading is reduced in half in an MEA with a conventional GDE anode. Since the kinetics of the ORR occurring at the cathode are slower and the cathode is the challenging electrode in terms of performance, it is reasonable that adding PAA to the

cathode would have a more significant effect on performance than adding PAA to the anode.

In addition to examining the difference in performance between the two GDE anode MEAs with Nafion or Nafion/PAA binder , the performance of the two conventional GDE anode MEAs were compared to an MEA with an electrospun nanofiber anode of weight ratio composition 65:23:12 Pt:Nafion:PAA at 0.10mg_{Pt}/cm^2 loading. The result of this comparison is shown in Figures 11 and 12. The polarization data shown in Figure 11 compares voltage vs. current density plots for the two MEAs with conventional GDE anodes of different compositions at 0.10 mg_{Pt}/cm^2 loading and an electrospun nanofiber anode MEA at an anode loading of 0.10 mg_{Pt}/cm^2. The MEA with the electrospun nanofiber anode displayed the highest current density (734 mA/cm^2) at 0.60V, as compared to 557 and 595 mA/cm^2 observed for the MEAs with GDE anodes of 65:23:12 Pt:Nafion:PAA and 70:30 Pt:Nafion composition, respectively. Although experimental data in Figure 10 indicated that the addition of PAA diminished MEA performance for conventional anode MEAs, an improvement in performance is seen when the fuel cell anode was an electrospun mat, where the nanofiber anode MEA outperformed conventional GDE anodes with and without PAA. Since a fuel cell may be operated at high voltage (low power) as well as maximum power, it is important to look at both the maximum power output of an electrode, as well as the power density at 0.6V (a often used standard voltage reported in the literature[20]). As shown in Figures 11 and 12, both the maximum power density and the power density at 0.6V are significantly higher in the electrospun nanofiber electrode than either of the decal electrodes. These results suggest that though the addition of PAA adversely affects electrode reaction rates

and power output in a fuel cell, this negative effect is overwhelmed by the positive benefits of a nanofiber anode morphology. So the beneficial structure of a nanofiber fuel cell cathode (intra and inter fiber porosity and a uniform distribution of catalyst and binder) as discussed by Brodt et al[25] contributes to a beneficial effect on the performance of a nanofiber anode which counterbalances the detrimental effect of PAA of MEA performance. The polarization curves also show that there is a lower slope in the ohmic region for the MEA with the nanofiber anode, which suggests that there is less ohmic resistance associated with a nanofiber anode. Since Brodt et al.[29] have shown that PAA increases the ohmic resistance of the binder, the higher slope of the nanofiber anode MEA curve in Figure 11 is tentatively attributed to less membrane/electrode contact resistance.

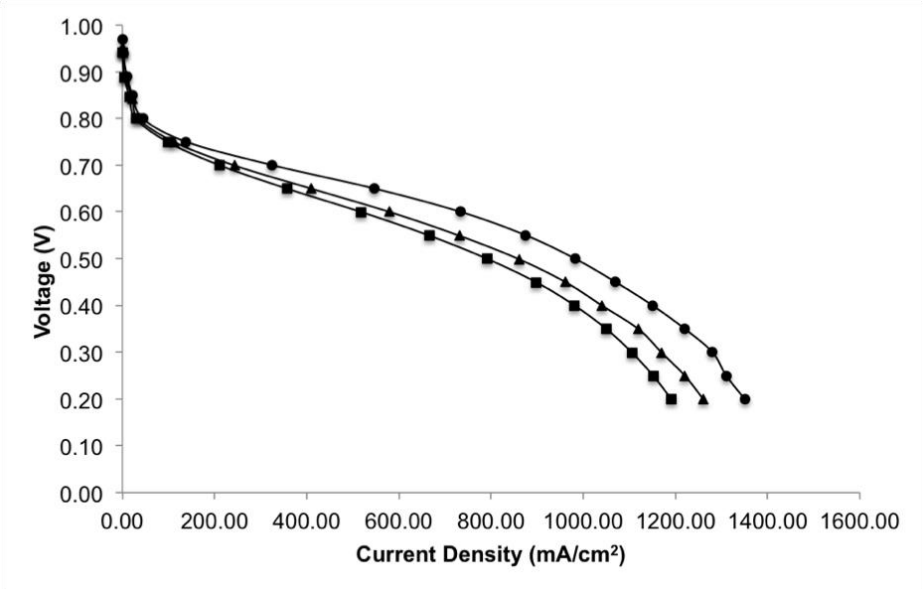

Figure 10. Polarization curves of three MEAs with different anodes and the same nanofiber cathode. (•) Electrospun nanofiber anode of 65:23:12 Pt:Nafion:PAA weight ratio, (▲) conventional GDE anode of 70:30 Pt:Nafion composition, and (■) conventional GDE anode of 65:23:12 Pt:Nafion:PAA composition. All MEAs contained anodes of 0.10 mg_{Pt}/cm^2 loading and an electrospun nanofiber cathode of 0.10 mg_{Pt}/cm_2

loading and 65:23:12 Pt:Nafion:PAA weight ratio composition. Fuel cell operating conditions: 80◦C, 100% RH feed gases at ambient pressure, 125 sccm H_2 and 500 sccm air.

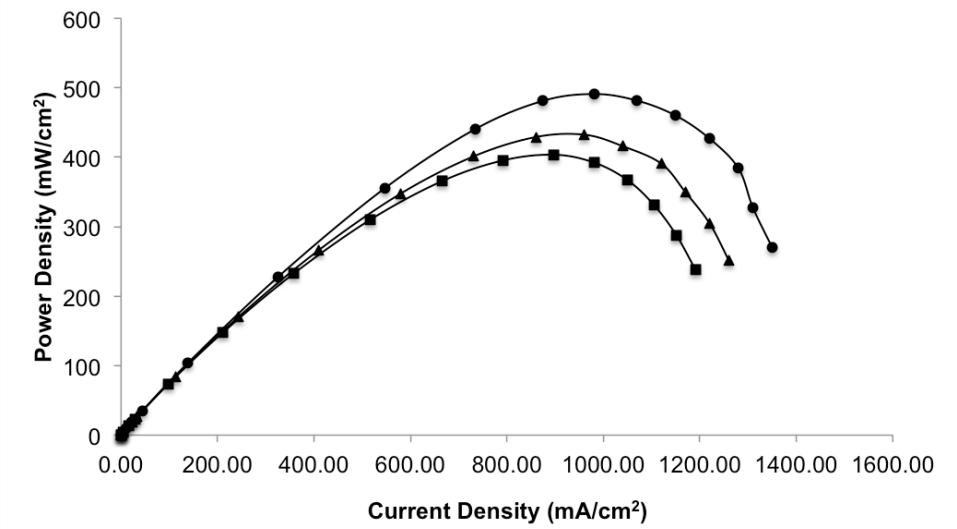

Figure 11. Power density vs. current density plots of three MEAs of different anodes. (•) Electrospun nanofiber anode of 65:23:12 Pt:Nafion:PAA weight ratio, (▲) conventional GDE anode of 70:30 Pt:Nafion composition, and (■) conventional GDE anode of 65:23:12 Pt:Nafion:PAA composition. All MEAs contained anodes of 0.10 mg_{Pt}/cm^2 loading and an electrospun nanofiber cathode of 0.10 mg_{Pt}/cm_2 loading and 65:23:12 Pt:Nafion:PAA weight ratio composition. Fuel cell operating conditions: 80◦C, 100% RH feed gases at ambient pressure, 125 sccm H_2 and 500 sccm air.

Referring to Figure 12, the maximum power density of the electrospun anode MEA was 491 mW/cm^2, while the maximum power density of the GDE-anode MEAs was lower: 432 mW/cm^2 when the GDE anode binder was Nafion and 403 mW/cm^2 when the GDE anode binder was Nafion+PAA. A more pronounced increase in performance with the electrospun anode MEA is observed at 0.6V. The power density of

the electrospun anode MEA at 0.6V is 440 mW/cm^2, while the power density of the standard GDE-anode MEA with Nafion and the GDE-anode MEA with Nafion+PAA binder are 347 mw/cm^2 (a 21% decrease from the electrospun anode) and 311 (29% decrease) mW/cm^2, respectively. The increase in power output for the MEA with a nanofiber anode is associated with an increase in electrochemically active Pt surface area, as was seen and discussed by M. Brodt et al.[25] in their paper on nanofiber fuel cell cathodes. Electrochemical surface area (ECSA) is the measure of the area of Pt that can actually be accessed by the reactant gases and can actually catalyze the HOR and ORR since isolated catalyst does not contribute to the electrochemical reactions. This increase in ECSA results in a higher rate of Pt utilization and is attributed to the unique nanofiber morphology where intra-fiber and inter-fiber porosity contribute to the increased ECSA.[25]

3.4 Effect of Pt Loading on MEA performance

In order to assess the effect of Pt loading on nanofiber anode MEA performance, five different MEAs were prepared with the following anode Pt loadings: 0.126, 0.101, 0.081, 0.046, and 0.026 mg_{Pt}/cm^2. All MEAs contained a Nafion 212 membrane and a nanofiber cathode with a Pt loading of 0.10 mg_{Pt}/cm^2. Fuel cell performance was assessed by comparing both voltage-current density polarization curves and power density (mW/cm^2) vs. current density (mA/cm^2) plots for each MEA. Hydrogen/air polarization data were collected at 80°C, 100% relative humidity, and ambient pressure, where the hydrogen and air flow rate were 125 sccm and 500 sccm air, respectively.

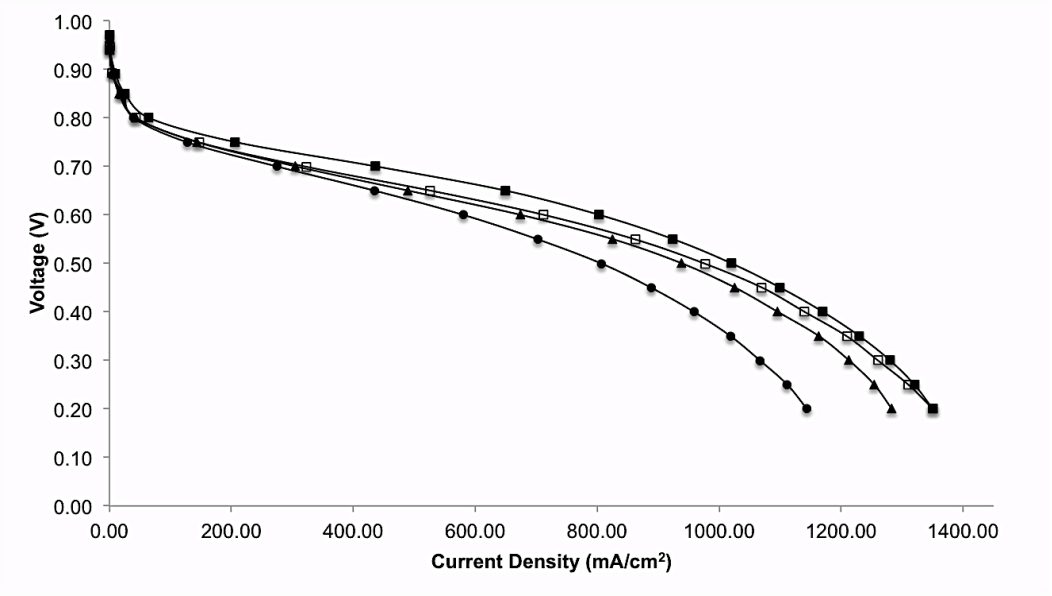

Figure 12. Polarization curves for 5 cm^2 MEAs with a Nafion 212 membrane, an electrospun cathode of Pt loading 0.10mg_{Pt}/cm^2, and electrospun anodes of varying Pt loading. The anode Pt loading was: (•) 0.026, (□) 0.046, (o) 0.081, (■) 0.101, and (▲) 0.126 mg_{Pt}/cm^2 Pt loading. Fuel cell operating conditions: 80◦C, 100% RH feed gases at ambient pressure, 125 sccm H_2 and 500 sccm air.

Figure 13 shows the polarization curves for the MEAs with four different anode Pt loadings. The highest current densities for the entire voltage range under investigation (approximately 0.20-1.0 V) were obtained when the nanofiber anode MEA Pt loading was 0.101 mg_{Pt}/cm^2. The MEA with an anode Pt loading of 0.126 mg_{Pt}/cm^2 exhibited less power (generally lower current densities at a given voltage) than either the 0.101 or 0.046 mg_{Pt}/cm^2 nanofiber anode MEAs, for reason not well understood at this time. However, it should be noted that for all MEAs tested with an anode Pt loading in the range of 0.046-0.126 mg_{Pt}/cm^2, the observed current densities in the high voltage range (>0.60V) were essentially the same and within experimental error (estimated to be 5-10%). The low power output for the MEA with an anode Pt loading of 0.026 mg/cm^2

was associated with a non-uniform density of fibers in the electrospun anode mat, due to the fact that the anode mat was very thin and natural fluctuations in fiber density deposition during electrospinning were accentuated in such tin mats. In future experiments, one should lower the Pt content in the electrospinning ink to achieve a Pt anode loading at/near/below 0.026 mg/cm^2.

Table 4. Current density at 0.6V for each anode of composition 65:23:12 Pt:Nafion:PAA and varied Pt loading for a 5cm^2 MEA with a Nafion 212 membrane, an electrospun cathode with Pt loading 0.10 mg$_{Pt}$/cm^2. Fuel cell operating conditions: 80◦C, 100% RH feed gases at ambient pressure, 125 sccm H_2 and 500 sccm air.

Pt Loading (mg$_{Pt}$/cm^2)	**Current Density at 0.60V (mA/cm^2)**
0.026	580
0.046	712
0.081	654
0.101	734
0.126	673

The power density ratio of MEAs with nanofiber anodes with 0.046 and 0.101 Pt loading, is 1.03 while the Pt loading ratio is 2.19. It is obvious from these results that the amount of Pt in a fuel cell nanofiber anode can be reduced by about half with essentially no loss in power density at cell voltages > 0.6 V.

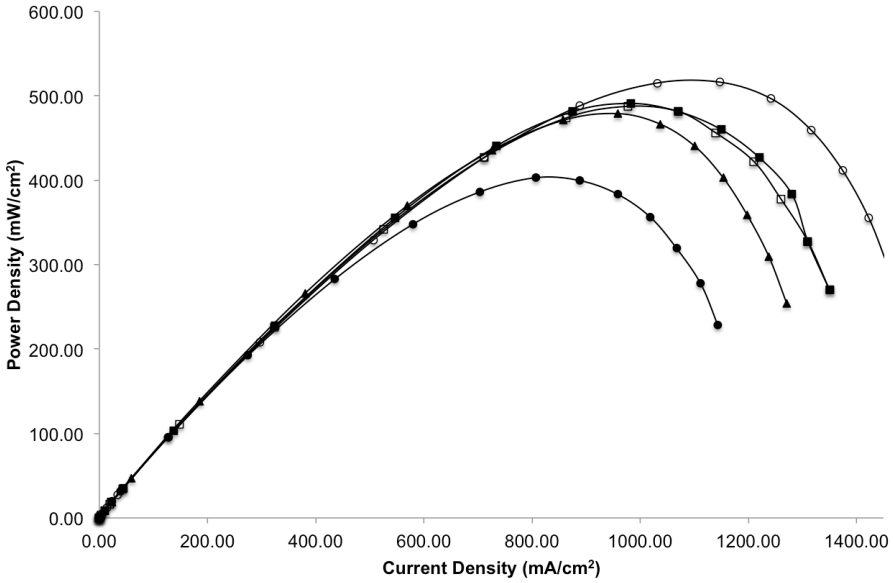

Figure 13. Plots of power density vs. current density for 5cm^2 MEAs with a Nafion 212 membrane, an electrospun cathode of Pt loading 0.10mg$_{Pt}$/cm^2, and electrospun anodes of varying Pt loading. The anode Pt loading was (•) 0.026, (□) 0.046, (o) 0.081, (■) 0.101, and (▲) 0.126 mg$_{Pt}$/cm^2 Pt loading. Fuel cell operating conditions: 80◦C, 100% RH feed gases at ambient pressure, 125 sccm H_2 and 500 sccm air.

Figure 14 shows the plots of power density vs. current density for MEAs of varying anode Pt loading and Table 5 lists the maximum power density achieved for each anode Pt loading. The power density ratio at max power for MEAs with 0.101 and 0.046 mg$_{Pt}$/cm^{2,} respectively, is 0.99 with a Pt loading ratio of 2.19. The power density ratios are effectively equal at 0.60V and max power. As shown in Figure 14, the plots of power density vs. current density almost completely overlap for the MEAs of 0.101 and 0.045 mg$_{Pt}$/cm^2 loading. The power output for these two MEAs are effectively the exact same with over a 200% decrease in the amount of Pt required over the entire voltage range. This is significant because it implies that regardless of the operating voltage in the fuel cell, the Pt loading in the anode can be cut in half without sacrificing power output.

Table 5. Maximum power densities for MEAs with a nanofiber anode of composition 65:23:12 Pt:Nafion:PAA and different anode Pt loadings for a 5cm^2 MEA with a Nafion 212 membrane, and an electrospun cathode with Pt loading 0.10 mg$_{Pt}$/cm^2. Fuel cell operating conditions: 80◦C, 100% RH feed gases at ambient pressure, 125 sccm H_2 and 500 sccm air.

Pt Loading (mg$_{Pt}$/cm^2)	Maximum Power Density (mW/cm^2)
0.026	403
0.046	488
0.081	516
0.101	482
.126	478

3.5 Cost Comparison For an Automotive Fuel Cell Stack

Based on the experimental data collected in this project, the amount of Pt required in a 80 kW automotive fuel cell stack was calculated for a nanofiber MEA, where the cathode Pt loading was held constant at 0.10 mg$_{Pt}$/cm^2 and the anode loading was varied from 0.026 to 0.126 mg$_{Pt}$/cm^2 (the same range of loadings as shown in Figure 13 and 14). Two scenarios were examined: a fuel cell stack based on the experimentally maximum power and the measured power output at 0.6 V. In the analysis, the cathode nanofiber Pt loading was fixed at 0.10 mg/cm^2. The results of these analyses are summarized in Tables 6 and 7.

Table 6. Grams Pt required for 80 kW nanofiber MEA stack operating at 0.60V for different anode Pt loadings, where the cathode loading was fixed at 0.10 mg_{Pt}/cm^2.

Pt Anode Loading (mg_{Pt}/cm^2)	**Power density at 0.60V (mW/cm^2)**	**Total g Pt Required for 80 kW stack**	**Anode g Pt Required for 80 kW stack**	**Stack Size (ft^2) required to generate 80 kW**
0.026	348	29	6	247
0.046	427	27	8.5	202
0.081	427	34	15.2	217
0.101	440	37	18.6	196
0.126	436	42	23.4	198

For fuel cell operation at 0.6 V (where fuel utilization is high), the lowest Pt loading is achieved when the stack utilizes a nanofiber anode with a Pt loading of 0.046 mg_{Pt}/cm^2 and a cathode of 0.10 mg_{Pt}/cm^2. If the anode Pt loading is increased to 0.101 mg_{Pt}/cm^2, the required Pt loading is increased from 27 g Pt required, but there is a decrease in the total required MEA area because fewer MEAs need to be stacked in order to contain the same amount of Pt and therefore generate the same amount of power in a fuel cell. According to a cost breakdown on fuel cell components published by the U.S. Department of Energy, the cost per component depends on the number of systems manufactured per year. At a rate of 1,000 systems/year, the cost of Pt catalyst comprises 16% of the cost of the fuel cell stack, whereas the membrane comprises 32% of the cost. On the contrary, at a rate of 500,000 systems/year, the Pt catalyst and membrane comprise 49% and 11% of the total cost of the stack, respectively.[28] Based on this and the experimental data collected, it depends on the number of systems manufactured what is more cost efficient in terms of Pt loading vs. stack size required. In a scenario where

500,000 systems are manufactured per year, the cost of Pt greatly outweighs the cost of the other fuel cell components, so decreasing the anode Pt loading to 0.046 mg_{Pt}/cm^2 from 0.101 mg_{Pt}/cm^2 and keeping the cathode Pt loading at 0.10 mg_{Pt}/cm^2 requires a larger fuel cell stack but a significant (55%) reduction in the amount of Pt required. On the contrary, if only 1000 systems are manufactured per year, the cost of the membrane comprises a much larger percentage of the cost of the fuel cell stack so it is necessary to keep the size of the fuel cell stack as small as possible.

Table 7. Grams Pt required for 80 kW nanofiber MEA stack operating at maximum power for different anode Pt loadings, where the cathode loading was fixed at 0.10 mg_{Pt}/cm^2.

Pt Anode Loading (mg_{Pt}/cm^2)	**Power density at max power (mW/cm^2)**	**Total g Pt Required for 80 kW stack**	**Anode g Pt Required for 80 kW stack**	**Stack Size (ft^2) required to generate 80 kW**
0.026	403	25	5.2	214
0.046	488	24	7.6	177
0.081	516	28	12.5	215
0.101	482	33	16.6	175
0.126	478	38	21.2	180

At maximum power (where the fuel utilization is low but the required MEA area in the stack is at a minimum), only 24 grams of Pt are needed for the 80 kW stack for a nanofiber anode with a loading of 0.046 mg_{Pt}/cm^2 and a cathode loading of 0.10 mg_{Pt}/cm^2. At maximum power, the amount of required Pt is decreased and the total MEA is decreased, as compared to the 0.6V case but highest conversion efficiency is achieved

at higher voltages[2] and as such, operating at lower voltages results in unwanted heating effects and extra fuel costs. Based on the experimental data, at 0.60V, the fuel cell stack required to generate 80 kW with an anode Pt loading of 0.046 mg_{Pt}/cm^2 is 177 sq ft, compared to 202 sq. ft. operating at max power (0.50V)—a 13% increase in the size of the fuel cell stack. In order to determine whether operating at max power or 0.60V is best in terms of cost, it would be necessary to experimentally determine the difference in operating cost at the two voltages. Since the long-term goal of PEM fuel cell research is mass commercialization and the cost of Pt far outweighs the cost of the other fuel cell stack components at higher rates of production, the scenario in which the least amount of Pt is utilized (0.046 mg_{Pt}/cm^2 anode).

3.6 Effect Of Temperature On Fuel Cell Performance

The effect of temperature on fuel cell performance was studied using an electrospun anode and cathode of 0.126 and 0.101 mg/cm^2 Pt loading, respectively. Only two temperatures were investigated, 40 and 80°C. As can be seen from the polarization curves in Figure 15 and the power density vs. current density plots in Figure 16, a significant improvement in performance is observed when the temperature is increased from 40°C to 80°C.

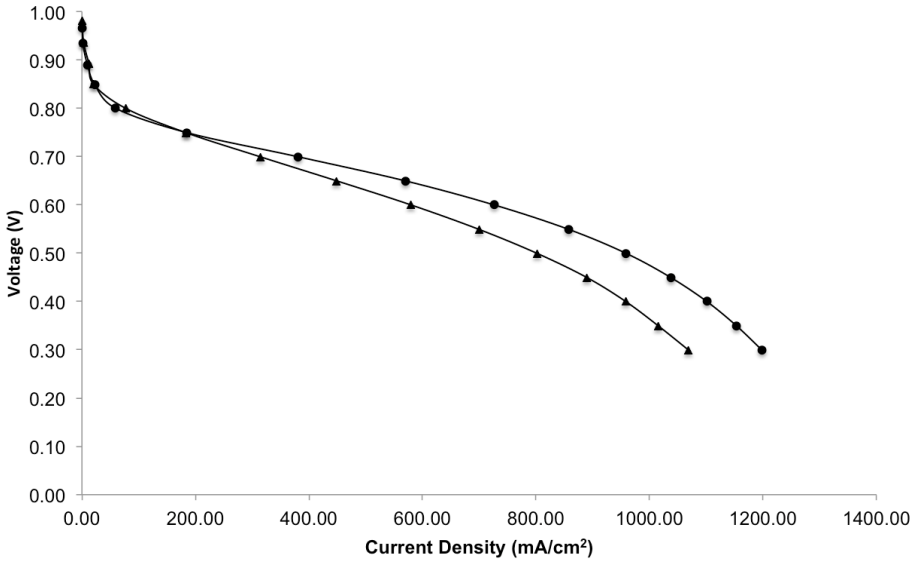

Figure 14. Polarization curves for a 5cm^2 MEA with a Nafion 212 membrane, an electrospun cathode and anode of 0.10 and 0.126 mg$_{Pt}$/cm^2 Pt loading, respectively at 40°C (▲), and 80°C(•). Fuel cell operating conditions: 100% RH feed gases at ambient pressure, 125 sccm H_2 and 500 sccm air.'

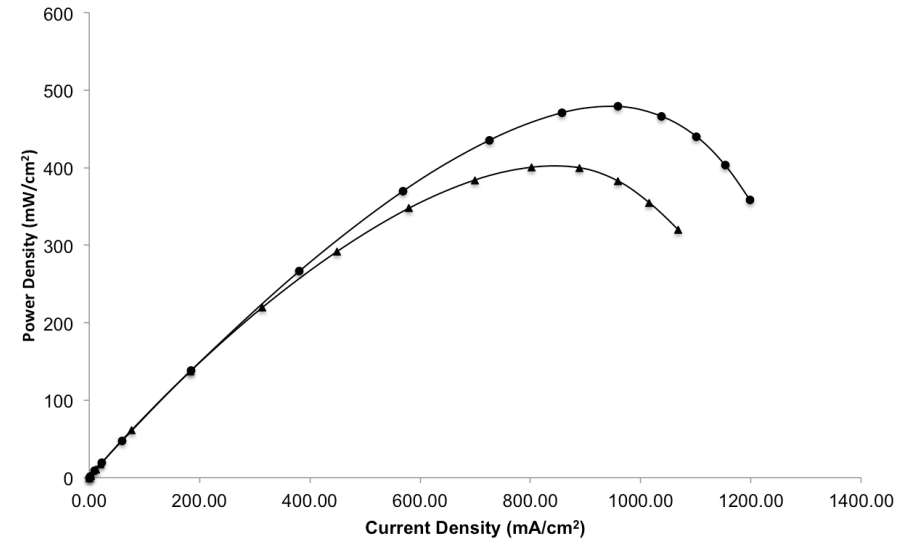

Figure 15. Polarization curves for a 5cm^2 MEA with a Nafion 212 membrane, an electrospun cathode and anode of 0.10 and 0.126 mg$_{Pt}$/cm^2 Pt loading, respectively at 40°C (▲) and 80°C (•). Fuel cell operating conditions: 100% RH feed gases at ambient pressure, 125 sccm H_2 and 500 sccm air.

The same trend was observed in by Brodt et al[25] in comparing fuel cell performance at 60°C and 80°C for an MEA with an electrospun cathode of 0.55 mg_{Pt}/cm^2 and electrospun anode of 0.56 mg_{Pt}/cm^2 loading. In this study, the max power observed was 400 and 450 mW/cm^2 for 60°C and 80°C, respectively. This compares logically to the results shown in Figure 16, where an increase from 400 to 478 mW/cm^2 is observed when the temperature is increased from 40°C to 80°C. In this case, the increase in power is proportional to the increase in temperature. Since these two studies are conducted using MEAs with electrodes of different Pt loadings, this data would suggest that the effect of temperature is independent of Pt loading, though a more extensive study would be required to determine the validity of this observation.

4 CONCLUSIONS

Based on the results found in this set of experiments, the following conclusions were drawn:

1. An MEA containing an electrospun nanofiber anode produced a higher power density compared to an MEA containing a conventional GDE anode at the same anode and cathode Pt loading (440 vs. 347 mW/cm^2 at 0.60V at 0.10 mg_{Pt}/cm^2 anode and cathode Pt loading). This is attributed to the higher electrochemical surface area with the nanofiber morphology, resulting in improved Pt utilization.
2. An electrospun nanofiber anode with a Pt Loading of 0.046 mg_{Pt}/cm^2 produced more power (488 vs. 347 mW/cm^2 at 0.60V) in a hydrogen/air fuel cell MEA (with a 0.10 mg_{Pt}/cm^2 cathode) than a conventional GDE anode at a Pt loading of 0.097 mg/cm^2). Experimental results indicate that the amount of Pt required in the anode can be cut in half using an electrospun fiber morphology.
3. Above a Pt loading of 0.05 mg_{Pt}/cm^2, no appreciable change in power density is observed in hydrogen/air fuel cell MEAs containing an electrospun nanofiber anode when the anode Pt loading is increased. The power density produced in the hydrogen/air fuel cell is effectively the same for MEAs containing electrospun nanofiber anodes of Pt loading 0.046-0.126 mg_{Pt}/cm^2.
4. A significant decline in power density is observed with an anode Pt loading of 0.026 mg_{Pt}/cm^2. This is attributed to a thinner electrode with poorer areal distribution and a lack of membrane surface coverage, thus providing insufficient catalyst contact.

5. Compared to the results published by Brodt et al[25], the effect of Pt loading on power density of electrospun anodes in hydrogen/air fuel cell MEAs is less significant than the effect of Pt loading on the cathode. This is attributed to the slower kinetics of the oxygen reduction reaction occurring at the cathode compared to the hydrogen oxidation reaction occurring at the anode.
6. The ability to achieve the same power density from an MEA with an anode containing half the amount of Pt in the electrospun anode corresponds to a dramatic 15g reduction in the amount of Pt required for an 80 kW fuel cell stack—a 70% reduction that would have a significant impact on the cost to manufacture a fuel cell vehicle.

5 SUGGESTIONS FOR FUTURE WORK

1. Attempts should be made to electrospin Nafion using high molecular weight polymers other than PAA. Three potential binders that could be used to replace PAA are polyvinylpirrolidone (PVP), polystyrene (PS), or polyvinyl alcohol (PVA), all of which have been electrospun with Nafion for use in membranes.[31-32] PAA has been shown to cause a decline in power density in a hydrogen/air PEM fuel cell, making it reasonable to assume that replacing PAA could improve power density.
2. Nanofiber anode mats with loadings of 0.02 to 0.05 mg_{Pt}/cm^2 should be prepared and tested using 20% Pt/C catalyst, rather than the 40% Pt/C used in the present studyThe lowered power density of an MEA with an electrospun nanofiber anode of Pt loading of 0.026 mg_{Pt}/cm^2 in a hydrogen/air fuel cell test was attributed to poor areal distribution and non-uniformity of fibers during electrospinning. The use of the lower Pt-content catalyst powder will double the amount of electrospun fiber for a given Pt loading and will increase the thickness and hopefully the areal uniformity of the mat, resulting in more intimate contact with the catalyst and thus improved power density.
3. Experiments should be done to prepare and test electrospun nanofiber electrodes using non-precious metal catalysts, such as electrospun polyaniline(PANI)-derived NMPC nanofibers. Although results show that the Pt can be reduced significantly at the anode, the overall amount of Pt required to generate enough power to power an automobile is still quite high. Since electrospun nanofibers have a greater electrochemical surface area and thus exhibit higher power density,

it is reasonable to assume that electrospinning electrospun polyaniline(PANI)-derived NMPC nanofibers would result in improved power density at a cheaper cost than expensive Pt-based electrodes.

REFERENCES

1. Dong, Z.; Kennedy, S. J.; Wu, Y., Electrospinning materials for energy-related applications and devices. *Journal of Power Sources* **2011,** *196* (11), 4886-4904.
2. Barbir, F.; Gomez, T., Efficiency and Economics of Proton Exchange Membrane (PEM) Fuel Cells. *Int. J. Hydrogen Energy* **1997,** *22* (10/11), 1027-1037.
3. Song, C., Fuel processing for low-temperature and high-temperature fuel cells: Challenges, and opportunities for sustainable development in the 21st century. *Catalysis Today* **2002,** *77*, 17-49.
4. Chen, J.; Siegel, J. B.; Matsuura, T.; Stefanopoulou, A. G., Carbon Corrosion in PEM Fuel Cell Dead-Ended Anode Operations. *Journal of The Electrochemical Society* **2011,** *158* (9), B1164.
5. Wang, J.; Yin, G.; Shao, Y.; Zhang, S.; Wang, Z.; Gao, Y., Effect of carbon black support corrosion on the durability of Pt/C catalyst. *Journal of Power Sources* **2007,** *171* (2), 331-339.
6. Barbir, F., *PEM Fuel Cells: Theory and Practice*. 2nd Edition ed.; Elsevier Inc: 1954; p 508.
7. He, C.; Desai, S.; Brown, G.; Bollepalli, S., PEM Fuel Cell Catalysts: Cost, Performance, and Durability *The Electrochemical Society Interface* **2005,** *Fall 2005*, 41-44.
8. Li, Q.; Jensen, J. O.; Savinell, R. F.; Bjerrum, N. J., High temperature proton exchange membranes based on polybenzimidazoles for fuel cells. *Progress in Polymer Science* **2009,** *34* (5), 449-477.
9. Gasteiger, H. A.; Kocha, S. S.; Sompalli, B.; Wagner, F. T., Activity benchmarks and requirements for Pt, Pt-alloy, and non-Pt oxygen reduction catalysts for PEMFCs. *Applied Catalysis B: Environmental* **2005,** *56* (1-2), 9-35.
10. Rismani-Yazdi, H.; Carver, S. M.; Christy, A. D.; Tuovinen, O. H., Cathodic limitations in microbial fuel cells: An overview. *Journal of Power Sources* **2008,** *180* (2), 683-694.
11. Energy, U. S. D. o. *Fuel Cell System Cost - 2013* 2013.
12. Meyers, J. P.; Darling, R. M., Model of Carbon Corrosion in PEM Fuel Cells. *Journal of The Electrochemical Society* **2006,** *153* (8), A1432.
13. Wilson, M. S.; Valerio, J. A.; Gottesfeld, S., Low Platinum Loading Electrodes For Polymer Electrolyte Fuel Cells Fabricated Using Thermoplastic Ionomers. *Electrochimica Acta* **1995,** *40* (3), 449-477.
14. Litster, S.; McLean, G., PEM fuel cell electrodes. *Journal of Power Sources* **2004,** *130* (1-2), 61-76.
15. Nørskov, J. K.; Rossmeisl, J.; Logadottir, A.; Lindqvist, L.; Kitchin, J. R.; Bligaard, T.; Jónsson, H., Origin of the Overpotential for Oxygen Reduction at a Fuel-Cell Cathode. *The Journal of Physical Chemistry B* **2004,** *108* (46), 17886-17892.
16. Bing, Y.; Liu, H.; Zhang, L.; Ghosh, D.; Zhang, J., Nanostructured Pt-alloy electrocatalysts for PEM fuel cell oxygen reduction reaction. *Chemical Society reviews* **2010,** *39* (6), 2184-202.

17. Wang, C.; Waje, M.; Wang, X.; Tang, J. M.; Haddon, R. C.; Yan, Proton Exchange Membrane Fuel Cells with Carbon Nanotube Based Electrodes. *Nano Letters* **2003,** *4* (2), 345-348.
18. Chen, Z.; Higgins, D.; Yu, A.; Zhang, L.; Zhang, J., A review on non-precious metal electrocatalysts for PEM fuel cells. *Energy & Environmental Science* **2011,** *4* (9), 3167-3192.
19. Wu, G.; More, K. L.; Johnston, C. M.; Zelenay, P., High-performance electrocatalysts for oxygen reduction derived from polyaniline, iron, and cobalt. *Science* **2011,** *332* (6028), 443-7.
20. Zhang, W.; Pintauro, P. N., High-Performance Nanofiber Fuel Cell Electrodes. *ChemSusChem* **2011,** *4* (12), 1753-1757.
21. Burke, L. D. & Murphy, O. J. Cyclic voltammetry as a technique for determining the surface area of RuO_2 electrodes. **96,** 19–27 (1979).
22. Doña Rodríguez, J. M., Herrera Melián, J. A. & Pérez Peña, J. Determination of the Real Surface Area of Pt Electrodes by Hydrogen Adsorption Using Cyclic Voltammetry. *J. Chem. Educ.* **77,** 1195 (2000).
23. Fisica, C. & Milano, U. Real surface area measurements. **63,** (1991).
24. Pozio, A., Francesco, M. De, Cemmi, A., Cardellini, F. & Giorgi, L. Comparison of high surface Pt / C catalysts by cyclic voltammetry. **105,** 13–19 (2002).
25. Brodt, M.; Wycisk, R.; Pintauro, P. N., Nanofiber Electrodes with Low Platinum Loading for High Power Hydrogen/Air PEM Fuel Cells. *Journal of the Electrochemical Society* **2013,** *160* (8), F744-F749.
26. Li, D.; Xia, Y., Electrospinning Nanofibers: Reinventing the Wheel? *Adv. Mater.* **2004,** *16* (14), 1151-1170.
27. Ballengee, J. B.; Pintauro, P. N., Preparation of nanofiber composite proton-exchange membranes from dual fiber electrospun mats. *Journal of Membrane Science* **2013,** *442*, 187-195.
28. Spendelow, J.; Marcinkoski, J. Fuel Cell System Cost- 2013. 1–8 (2013).
29. Brodt, M.; Wycisk, R.; Pintauro, P.; Han, T.; Dale, N; Niangar, E;, Adjemian, K., Fabrication, In-Situ Performance, and Durability of Nanofiber Fuel Cell Cathodes. *J. Electrochem. Soc.* (in preparation)
30. Chen, H.; Snyder, J. D.; Elabd, Y. A., Electrospinning and Solution Properties of Nafion and Poly(acrylic acid) *Macromolecules* 2008, 41, (1), 128-135.
31. Carbone A.; Saccà A.; Busacca C.; Frontera P.; Antonucci P.; Passalacqua E. Nafion electro-spun reinforced membranes for polymer electrolyte fuel cell. *J Nanosci Nanotechnol* **2011**, *11*, 10, 8768-74.
32. Lin, H; Wang, S; Chiu, C; Yu, T; Chen, L; Preparation of Nafion/poly(vinyl alcohol) electro-spun fiber composite membranes for direct methanol fuel cells, *Journal of Membrane Science* **2010**, *365*, 114-122. Volume 365, Issues 1–2, 1 December 2010, Pages 114-122